

Reconstructed Brain Like Neural Network R-KFDNN

Zhu Rongrong, Fudan University, Shanghai, China
rongrongzhu1969@163.com

ABSTRACT

Through the neural system damage and repair process of human brain, we can construct the complex deep learning and training of the repair process such as the damage of brain like high-dimensional flexible neural network system or the local loss of data, so as to prevent the dimensional disaster caused by the local loss of high-dimensional data. How to recover and extract feature information when the damaged neural system (flexible neural network) has amnesia or local loss of stored information. Information extraction generally exists in the distribution table of the generation sequence of the key group of the higher dimension or the lower dimension to find the core data stored in the brain. The generation sequence of key group exists in a hidden time tangent cluster. Brain like slice data processing runs on different levels, different dimensions, different tangent clusters and cotangent clusters. The key group in the brain can be regarded as the distribution table of memory fragments. Memory parsing has mirror reflection and is accompanied by the loss of local random data. In the compact compressed time tangent cluster, it freely switches to the high-dimensional information field, and the parsed key is buried in the information.

Keywords: Brain like, Nervous system injury and repair, Flexible neural network, Key group generation sequence, High-dimensional information field, Memory analysis

1. INTRODUCTION

Flexible depth neural network (KDNN) with unipolar and multipolar flexible weakly nonlinear clustering functions with parameters is designed, and it is that corresponding learning algorithm. Different from the ordinary neighborhood depth neural network (KDNN), KDNN can not only learn the connection weight, but also learn the parameters of flexible weakly nonlinear clustering function. Therefore, it can generate appropriate weak nonlinear clustering function morphology for each hidden layer and output layer unit according to the learning sample set. Flexible neural network can improve the performance of kdnn network and solve the classification and prediction problems in different fields.

From non flexible depth neural network (KFDNN) to flexible depth neural network (KFDNN), and then from flexible depth neural network (KFDNN) to brain like neural network; The relationship between hypersection of brain like heavy nucleus boundary key group generation sequence, flexible depth neural network (KFDNN) and brain like neural network is constructed.

1.1 Flexible neural network mathematical model

$$\forall K_{DNN}^{n-1}(\rho_{\lambda}^n, \theta^{\lambda}) \xrightarrow{k \text{ Iterations}} \exists K_{DNN}^{n-1}(\rho_{\lambda}^m, \theta^k \otimes \beta^k), \text{ if } \theta \otimes \beta, \rho \text{ and appearing weak nonlinearity}$$
$$S^{m+k-1} \left[(\rho^m \otimes \theta^k)^+ \wedge (\rho^m \otimes \theta^k)^- \right] \xrightarrow[\text{(Superball, Hypersp here)}]{\text{Left, right hemisp heres}} \left[S_{left}^{m+k-1}(\rho^m \otimes \theta^k)^+ \right] \wedge \left[S_{right}^{m+k-1}(\rho^m \otimes \theta^k)^- \right] \quad (1)$$

1.2 Mathematical model of brain like neural network analysis

Its core core is the left and right brain heavy nuclei of high-dimensional supersymmetric hypersurface normal complex variable high-dimensional tangent bundle.

$$1,2 S_{M_{\theta}}^{\omega(\theta)+1} \sim 1,2 S_{M_{\theta}(\exp)}^{\omega(\theta)+1} \xrightarrow[\text{brain like heavy nucleus}]{\text{Left and right,}} \left({}^+ \Omega_{t(\theta)}^{S_{\partial M}^{-1}} \wedge {}^- \Omega_{t(\theta)}^{S_{\partial M}^{-1}} \right) \quad (2)$$

The left and right brain heavy nuclei are substituted into the mathematical model of flexible neural network, then

$$S_{Left}^{m+k-1} \left({}^+ \Omega_{t(\theta)}^{S_{\partial M}^{-1}} \right) \wedge S_{Right}^{m+k-1} \left({}^- \Omega_{t(\theta)}^{S_{\partial M}^{-1}} \right) \simeq S_{Left}^{m+k-1} \left({}^+ \Omega_{t(\theta)}^{S_{\partial M}^{-1}} (\rho^t \otimes \theta^k) \right) \wedge S_{Right}^{m+k-1} \left({}^- \Omega_{t(\beta)}^{S_{\partial M}^{-1}} (\rho^t \otimes \beta^k) \right)$$

The relationship and evolution between the formation of neurons and K iterations.

if $\rho \rightarrow 1, \theta = 2k\pi + \theta_1 + \theta_2 + \dots, t \in \forall \sigma, (S_{\partial M}^{-1})^k$, then

$$S_{Left}^{m+k-1} \left({}^+ \Omega_{t(\theta)}^{(S_{\partial M}^{-1})^k} (\theta^k) \right) \wedge S_{Right}^{m+k-1} \left({}^- \Omega_{t(\beta)}^{(S_{\partial M}^{-1})^k} (\beta^k) \right) \cong S_{Left, Right}^{m+k-1} \left({}^+ \Omega_{t(\theta \wedge \beta)}^{S_{\partial M}^{-1}} (\theta^k \otimes \beta^k) \right) \quad (3)$$

The distribution of left and right hemispheres (brain like) is delayed. Perform a mathematical model to analysis of the effect.

The weak nonlinear fluctuation of information field is formed on the t' tangent disturbance of θ^k, β^k . The internal law can be observed by combining the above formula.

i. The iterative hyper slice kernel and high-dimensional time tangent perturbation kernel are analyzed.

$$[\pm S_{\partial M}^{-k}(\theta^k \wedge \beta^k)], {}^\pm \Omega' [t(\theta) \wedge t(\beta)]_{\partial}^k$$

ii. The time tangent problem of the hypercut kernel of the left and right brain (brain like).

$$\begin{array}{ccccc} S_{\partial M}^{-k}(\theta^k) & \longrightarrow & \Omega' [t^k(\theta)]_{\partial M} & & S_{\partial^2 M}^{-k}(\theta^k(t')) \\ \downarrow & & \downarrow & \longrightarrow & \downarrow \\ S_{\partial M}^{+k}(\beta^k) & \longrightarrow & \Omega' [t^k(\beta)]_{\partial M} & & S_{\partial^2 M}^{-k}(\beta^k(t')) \end{array}$$

The time tangent perturbation structure of left and right brain (brain like) overweight nuclei is called neurons for short.

Then $_{Left} S_{\partial^2 M}^{-k}(\theta^k(t')), _{Right} S_{\partial^2 M}^{-k}(\beta^k(t'))$. Therefore, neurons in the left and right brain (brain like) have different division of labor and operate in the dimension of time tangent, that is, information storage, operation, extraction, analysis and so on.

iii. How neurons are distributed in the sulcus of the left and right brain (brain like).

$${}^{1,2} S_{M_{\partial}(exp)}^{\omega(\theta)+1} [S_{\partial^2 M}^{-k}(\theta^k(t')) \wedge S_{\partial^2 M}^{-k}(\beta^k(t'))]$$

That is, sulcus gyrus causes brain like distribution dimension + 1, Moreover, the distribution of neurons presents the morphological characteristics of cooperative operation of probability distribution. Therefore, the human brain has the reason of changeable and innovation. The repair of the injured nervous system of the local nerve of the human brain is similar to that of the brain like nervous system, that is, the loss of local data of memory leads to amnesia; But it will not cause dimensional disaster of high-dimensional information field, The lead of memory restoration, that is, the time tangent between neurons, links the information of all dimensions.

$${}^{1,2} S_{M_{\partial}(exp)}^{\omega(\theta)+1} \left[[S_{\partial^2 M}^{-k}(\theta^k(t') \wedge \theta_{\partial}(t'))] \wedge [S_{\partial^2 M}^{-k}(\beta^k(t') \wedge \beta_{\partial}(t'))] \right],$$

Local missing function analysis of human brain (brain like) information data.

$${}^{1,2}S_{M_{\partial}^{(exp)}}^{\omega(\theta)+1} \partial (\wedge \theta_{\partial} (t')) \wedge {}^{1,2}S_{M_{\partial}^{(exp)}}^{\omega(\theta)+1} \partial (\wedge \beta_{\partial} (t')) \sim {}^{1,2}S_{M_{\partial}^{(exp)}}^{\omega(\theta)+1} \partial (\wedge \theta_{\partial} (t') \wedge \wedge \beta_{\partial} (t'))$$

$${}^{1,2}S_{M_{\partial}^{(exp)}}^{\omega(\theta)+1} \partial (\wedge \theta_{\partial} (t') \wedge \wedge \beta_{\partial} (t')) \simeq {}^{1,2}S_{M_{\partial}^{(exp)}}^{\omega(\theta)+1} \partial (\theta'_{\partial}(t')) , then$$

$$\exists \left[{}^{1,2}_{\partial M_{\partial}^{(exp)}} [\omega(\theta)+1] (\theta'_{\partial^2}(t')) \right]_{lost\ data}^{Brain\ like\ Drop\ 2\ dimensions} = \exists \left[{}^{1,2}_{M_{\partial}^2(exp)} [\omega(\theta)+1] (\theta'_{\partial^2}(t')) \right]$$

if $t' \rightarrow -\infty$, then , and non-existent data caused total amnesia.

iv. Neurons are accompanied by left and right brain damage (local), structural morphology.

$${}^{1,2}S_{M_{\partial}^{(exp)}}^{\omega(\theta)+1} \left[S_{\partial^2 M}^{-k} (\theta^k (t')) \wedge S_{\partial^2 M}^{-k} (\beta^k (t')) \right] - \left[{}^{1,2}_{M_{\partial}^2(exp)} [\omega(\theta')+1] (\theta'_{\partial^2}(t')) \right]_{lost}$$

$$\int \left[{}^{1,2}_{M_{\partial}^{(exp)}} [\omega(\theta)+1] (\theta'_{\partial}(t')) \right]_{lost} \text{ Repair data from the perspective of mathematical model.}$$

v. Data characteristics of neurons (left and right brain (brain like)) repairing local damage.

$$\int {}^{1,2}S_{M_{\partial}^{(exp)}}^{\omega(\theta)+1} \left[S_{\partial M}^{-k} (\theta^k (t')) \wedge S_{\partial M}^{-k} (\beta^k (t')) \right] + \int \left[{}^{1,2}_{M_{\partial}^{(exp)}} [\omega(\theta')+1] (\theta'_{\partial}(t')) \right]_{lost}$$

$$= \sum {}^{1,2}S_{M_{\partial}^{(exp)}}^{\omega(\theta)+1} \left[S_{\partial M}^{-k} (\theta^k (t') \oplus \theta'_{\partial}(t')) \wedge S_{\partial M}^{-k} (\beta^k (t') \oplus \theta'_{\partial}(t')) \right]$$

$${}^{1,2}S_{M_{\partial}^{(exp)}}^{\omega(\theta)+1} \left[S_{\partial^2 M}^{-k} (\theta^k (t')) \wedge S_{\partial^2 M}^{-k} (\beta^k (t')) \right]$$

$$= \sum {}^{1,2}S_{M_{\partial}^{(exp)}}^{\omega(\theta)+1} \left[S_{\partial M}^{-k} (\theta^k (t') \oplus \theta'_{\partial}(t')) \wedge S_{\partial M}^{-k} (\beta^k (t') \oplus \theta'_{\partial}(t')) \right] \quad (4)$$

Therefore, the repair of human brain (brain like) damage is generally distributed and obtained in the time tangent angle, that is, the relationship between dimension reduction and dimension increase of data. At the same time, there is the relationship between partial differential and integral (local) $\sum \theta'_{\partial}(t')$.

vi. The repair forms of local nerves in the left and right brain of human brain are different. Please observe the following formula.

$$\begin{cases} + \\ \Omega_M^{\partial} (\theta^k (t') \oplus \theta'_{\partial}(t'))_{Left} \\ - \\ \Omega_M^{\partial} (\beta^k (t') \oplus \theta'_{\partial}(t'))_{right} \end{cases}$$

Therefore, the left and right brain can cooperate to repair the local nervous system and restore the amnesia to normal.

$$\partial \Omega_M^k [\theta^k \beta^k (t') \oplus \theta'_{\partial}(t')] = \Omega_M^{k+1} [\theta(\rho(t))]$$

Therefore, the coordination of left and right brain (brain like) can better develop the brain and is also conducive to the repair of brain injury.

$$S_{Left}^{m+k-1} \left(+ \Omega_{t'(\theta \wedge \beta)}^{(S_{\partial M}^{-1})^k} (\theta^k \wedge \beta^k) \right) \cong \Omega_M^{k+1} [\theta(\rho(t))]_{S_{left, right}^{m+k-1}} \quad (5)$$

1.3 The Human brain (brain like) perceives the surrounding information field (assuming Similar MR information).

$$\Omega^{k+1} \left[\theta \left(\rho(t(MR)) \right) \right] = \Omega^{k+1} \left[\theta \left(\rho_t \left(\sum \frac{\delta}{\omega_i} \times \log |I + R^{-1} \times H_{ij} \times Q_{MR}^{Core \ energy} \times H_{ji}^H| \right) \right) \right], \text{ and}$$

$$R^{-1} \text{ interference signal}, Q_{MR}^{Core \ energy} = \text{Matrix} \begin{bmatrix} E_{X_E}^K \otimes X_K^H & & \\ & E_{X_S}^K \otimes X_K^H & \\ & & E_{X_M}^K \otimes X_K^H \end{bmatrix}_i^Q \quad (6)$$

i. The eye perception image of the human brain is equivalent to how signal of $MR^{H_{ij} \ Q_i \ H_{ji}^H}$ is processed in brain space.

The energy wave structure equation of human brain (brain like) supporting information field.

$$\Omega^{k+1} \left[\theta \left(\rho \left(t(Q_{MR}^{Core \ energy}) \right) \right) \right] = S_{Left}^{m+k-1} \left({}^{+\Omega(S_{\partial M}^{-1})^k}_t \left(\theta \wedge \beta (Q_{MR}^{Core \ energy}) \right) \right)$$

ii. The vector motion of energy fluctuation on the brain space surface (X_K^H) , so the above formula can be written as.

$$\Omega^{k+1} \left[\theta \left(\rho_t \left(\text{Matrix} \begin{bmatrix} E_{X_E}^K \otimes X_K^H & & \\ & E_{X_S}^K \otimes X_K^H & \\ & & E_{X_M}^K \otimes X_K^H \end{bmatrix}_i^Q \right) \right) \right]$$

$$= S_{Left}^{m+k-1} \left({}^{+\Omega(S_{\partial M}^{-1})^k}_t \left(\theta \wedge \beta (Q_{MR}^{Core \ energy}) \right) \left(\theta^k \wedge \beta^k \left(\text{Matrix} \begin{bmatrix} E_{X_E}^K \otimes X_K^H & & \\ & E_{X_S}^K \otimes X_K^H & \\ & & E_{X_M}^K \otimes X_K^H \end{bmatrix}_i^Q \right) \right) \right) \quad (7)$$

It can be seen from the above that the brain carries special energy waves and processes various signals in a higher dimension.

$$\Omega^{k+1} \left[\theta \left(\rho_t \left(\text{Matrix} \begin{bmatrix} E_{X_E}^K \otimes X_K^H & & \\ & E_{X_S}^K \otimes X_K^H & \\ & & E_{X_M}^K \otimes X_K^H \end{bmatrix}_i^Q \right) \right) \right] \rightarrow$$

$$\left(\frac{1}{4} \right)^{n-1} \times \sqrt{2} \left[\sin \left(\frac{\theta_1}{2} + \frac{\pi}{4} + n \cdot \frac{\pi}{4} \right) \cos \left(\sum_{i=2}^m \theta_i + \sum_{i=2}^m i \cdot \frac{\theta_i}{2} \right) \right.$$

$$\left. - \sin \left(\frac{\beta_1}{2} + \frac{\pi}{4} + n \cdot \frac{\pi}{4} \right) \cos \left(\sum_{i=2}^m \beta_i + \sum_{i=2}^m i \cdot \frac{\beta_i}{2} \right) \right]_{\theta \wedge \beta(t')}$$

Using the image definition function kernel of MR and integrating the right structure of the above formula, we can observe the polar coordinate image with higher dimension. And reference to Figure 1.

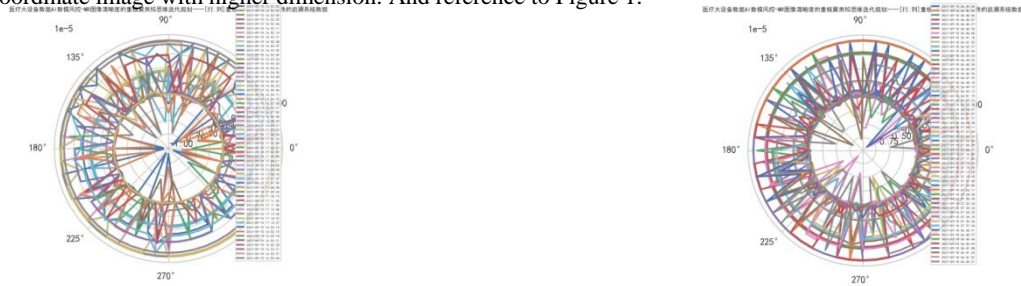


Figure 1. Higher dimensional MR image sharpness kernel function polar image.

iii. Perceive the fluctuation regular of MR information field in a higher dimension. ω_i is the angular velocity ($\omega_i = TR \otimes$

TE) High frequency wave angular velocity: $\omega_i(\delta^{-1})$, High frequency wave carrying image information.

$$\begin{aligned} \omega_i^{-1}(\delta) \times \log(H_{ij} \times Q_{MR}^{Core\ energy} \times H_{ji}^H) &= \frac{\log(H_{ij} \times Q_{MR}^{Core\ energy} \times H_{ji}^H)}{\omega_i(\delta)} \\ \frac{\theta}{\rho(t)} &= \frac{\log(H_{ij} \times Q_{MR}^{Core\ energy} \times H_{ji}^H)}{\omega_i(\delta)}, \quad \theta \times \omega_i(\delta) = \rho(t) \times \log(H_{ij} \times Q_{MR}^{Core\ energy} \times H_{ji}^H) \\ \Omega^{k+1}(\theta \cdot \rho_t(Q_{MR}^{Core\ energy})) &\rightarrow \frac{1}{(k+1)k(k-1)\dots} \times S_{Left, right}^{m+k-1}(\theta_t^k)_{\rho \rightarrow \delta} \\ \theta &= \frac{\rho(t)}{\omega_i(\delta)} \times \log(H_{ij} \times Q_{MR}^{Core\ energy} \times H_{ji}^H) \text{ is substituted into the above formula, then} \\ \frac{1}{(k+1)k(k-1)\dots} \times S_{Left, right}^{m+k-1} &\left(\frac{\rho(t)}{\omega_i(\delta)} \times \log(H_{ij} \times Q_{MR}^{Core\ energy} \times H_{ji}^H) \right)_{\partial}^k, \text{ and if } m \rightarrow 0, t', \text{ then} \\ [_{Left} S_{\partial^2 M}^{-k}(\theta^k(t')) \wedge_{right} S_{\partial^2 M}^{-k}(\beta^k(t'))] & \\ = \frac{1}{(k+1)k(k-1)\dots} \times S_{Left, right}^{m+k-1} &\left(\frac{\rho(t)}{\omega_i(\delta)} \times \log(H_{ij} \times Q_{MR}^{Core\ energy} \times H_{ji}^H) \right)_{\partial}^k \end{aligned} \quad (9)$$

Equation (9) above is the functional equation of the dimensionality reduction process of high-frequency wave carrying image information field.

vi. KFDNN has a dimension reduction process (gradient descent) in neural network training and learning.

If $\omega_i(\delta)$ high-frequency wave and brain like (human brain) wave have some low-frequency co vibration resonance, it will make the human brain uncomfortable, that is

$$\begin{aligned} \frac{(k+1)k(k-1)\dots}{\omega_i(\delta^{-1})} \times (S^{-k+1}) &\rightarrow \frac{\omega_i(\delta)}{(k+1)k(k-1)\dots} \times S_{Left, right}^{k-1}(Q_{MR}^{Core\ energy}) \\ \frac{\omega_i(TR \otimes TE)}{(k+1)k(k-1)\dots} \times S_{Left, right}^{k-1} &(Q_{MR}^{Core\ energy})_{\delta}^H \end{aligned}$$

The above function structure is the form of low-frequency co vibration resonance wave carrying image information.

$$\begin{aligned} S_{Left, right}^{-k+1}(Q_{MR}^{Core\ energy})_{\delta}^H &= \frac{\omega_i^{-1}(TR \otimes TE)}{(k+1)k(k-1)\dots} \times \left[\cos\left(\sum_{i=2}^m \theta_i + \sum_{i=2}^m i \cdot \frac{\theta_i}{2}\right) - \cos\left(\sum_{i=2}^m \beta_i + \sum_{i=2}^m i \cdot \frac{\beta_i}{2}\right) \right], \\ \text{and } \delta \rightarrow 1, \text{ or } \delta \rightarrow -\infty & \end{aligned} \quad (10)$$

$$\begin{aligned} S_{Left, right}^{-k+1}(Q_{MR}^{Core\ energy})_{\delta}^H &= \frac{\left(\frac{1}{4}\right)^n}{(k+1)k(k-1)\dots} \times \left[\sin\left(\theta_i + \sum_{i=2}^m \theta_i + n \cdot \frac{\pi}{4}\right) + \sin\left(\theta_i - \sum_{i=2}^m \theta_i + n \cdot \frac{\pi}{4}\right) \right], \\ \frac{(k+1) + k(k-1) + \dots}{\left(\frac{1}{4}\right)^n \times (k+1)k(k-1)\dots \times \omega_i(TR \otimes TE)} &= \frac{\left[\sin\left(\theta_i + \sum_{i=2}^m \theta_i + n \cdot \frac{\pi}{4}\right) - \sin\left(\theta_i - \sum_{i=2}^m \theta_i + n \cdot \frac{\pi}{4}\right) \right]}{\left[\cos\left(\sum_{i=2}^m \theta_i + \sum_{i=2}^m i \cdot \frac{\theta_i}{2}\right) - \cos\left(\sum_{i=2}^m \beta_i + \sum_{i=2}^m i \cdot \frac{\beta_i}{2}\right) \right]} \end{aligned}$$

$$\frac{(k+1) + k(k-1) + \dots}{\omega_i (TR \otimes TE)} \approx \frac{\left[\sin\left(\theta_i + \sum_{i=2}^m \theta_i + n \cdot \frac{\pi}{4}\right) + \sin\left(\theta_i - \sum_{i=2}^m \theta_i + n \cdot \frac{\pi}{4}\right) \right]}{\left[\cos\left(\sum_{i=2}^m \theta_i + \sum_{i=2}^m i \cdot \frac{\theta_i}{2}\right) - \cos\left(\sum_{i=2}^m \theta_i + \sum_{i=2}^m i \cdot \frac{\theta_i}{2}\right) \right]}$$

$$\frac{1}{\omega_i (TR \otimes TE)} \xrightarrow{\text{reduction}} \frac{\left[\sin\left(\theta_i + \sum_{i=2}^m \theta_i + n \cdot \frac{\pi}{4}\right) + \sin\left(\theta_i - \sum_{i=2}^m \theta_i + n \cdot \frac{\pi}{4}\right) \right]}{\lambda_i \left[\cos\left(\theta_i + \sum_{i=2}^m \theta_i\right) - \sin\left(\theta_i - \sum_{i=2}^m \theta_i + n \cdot \frac{\pi}{4}\right) \right]} \times \text{tg}\left(\sum \theta_i\right)$$

$$\frac{1}{\omega_i (TR \otimes TE)} = \text{ctg}\left(\sum_{i=2}^m i \cdot \frac{\theta_i}{2}\right), \therefore$$

$$S_{Left, right}^{-k+1}(Q_{MR}^{Core \ energy})_{\delta}^H = \text{ctg}\left(\sum_{i=2}^m i \cdot \frac{\theta_i}{2}\right)_{E_X} \quad (11)$$

The following and reference to Figure 2. (formula (11)) shows the brain like (left and right brain of human brain) of the three-dimensional image of the reduced resonance wave morphological equation of low-frequency co vibration carrying

image information. $S_{Left, right}^{-k+1}(Q_{MR}^{Core \ energy})_{\delta}^H$

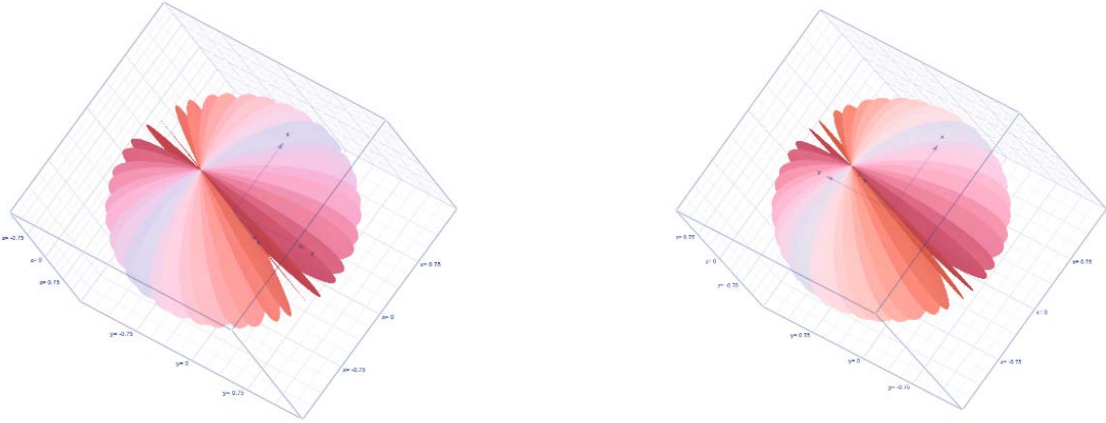


Figure 2. Three dimensional image of reduced resonance wave morphological equation of brain like with image information.

The left and right brain (brain like) kernels cooperate with the transformation of the fitting equation carrying the information reduced wave form.

$$+\Omega_{t'(\theta \wedge \beta)}^{(S_{\theta M}^{-1})^k}(\theta^k \wedge \beta^k) \sim \sum_{k \geq 3} S_{Left, right}^{-k+1}(Q_{MR}^{Core \ energy})_{\delta}^H, \text{ if } S_{Left, right}^{-k+1} \subset \text{ctg}\left(\sum_{i=2}^m i \cdot \frac{\theta_i}{2}\right)_{E_X} \quad (12)$$

Each reduced S^{-1} -slice stores a large amount of information, including information fragments similar to MR images. On the whole, it is a high-dimensional data of massive information stored in the brain-like(human brain). And there is a higher dimension information of the key group to extract the information, which is called the distribution table group of high dimension information. It is equivalent to the generation sequence of key group, so equation (5) is simplified to

$$S_{Left, right}^{m+k-1}\left(\sum_{k \geq 3} S_{Left, right}^{-k+1}(Q_{MR}^{Core \ energy})_{\delta}^H\right) \sim S_{Left, right}^{m+k-1}\left(\sum_{k \geq 3} \text{ctg}^s\left(\sum_{i=2}^m i \cdot \frac{\theta_i}{2}\right)_{E_X(t')}\right), \text{ and } s \text{ is expressed dimension}$$

$$S_{Left, right}^{m+k-1} \left(\sum_{k \geq 3}^m S_{Left, right}^{-k+1} (Q_{MR}^{Core \ energy})_{\delta}^H \right) \sim S_{Left, right}^{m+k-1} \left(\sum_{k \geq 3}^m ctg^s \left(\sum_{\rho=2}^m \rho_{\theta} \cdot \frac{\theta_{\rho(t')}}{2} \right)_{E_X(t')}^{Q_{MR}} \right), \text{ and}$$

$s \geq 3$ is expressed dimension, $\rho(t')$ is the polar diameter of polar coordinates, t' is the time tangent (13)

The key group generates the sequence $\left({}^+ \Omega_{t'(\theta)}^{S_{\partial M}^{-1}} \wedge {}^- \Omega_{t'(\theta)}^{S_{\partial M}^{-1}} \right)$ to the left and right brain (brain like) kernels, and cooperates with and carries the information to reduce the fluctuation fitting transformation (formula (13)). A large amount of information (such as MR image information) is stored on each reduced S^{-1} , and the extraction of information requires the generation sequence of key group, i.e. distribution table group (guidance), which may have a cotangent timeline $\rho_{\theta}(t')$.

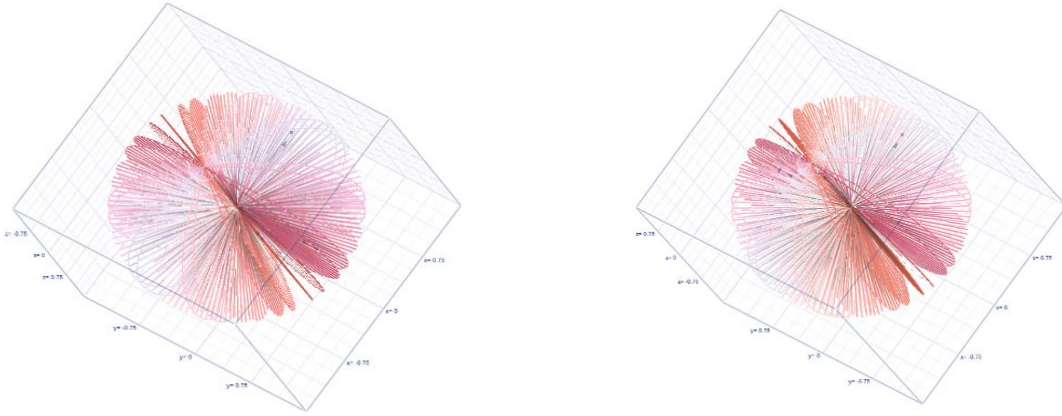


Figure 3. The generation sequence of the key group of each piece of S^{-1} information has a cotangent time line $\rho_{\theta}(t')$.

In the high-dimensional information field, there is a hidden timeline $\rho_{\theta}(t')$, and reference to Figure 3. that is, Cotangent bundle. It crosses the high-dimensional and low-dimensional brain like hypersections and S_k^{-1} -slice bundles, so it can be found that there may be the generation sequence of key groups in both brain like and human brain, and $\rho_{\theta}(t')$ cotangent bundle and S_k^{-1} slice bundle.

$$S_{Left, right}^{m+k-1} \left[\sum_{k \geq 3}^m ctg^s \left(\sum_{\rho=2}^m \rho_{\theta} \left(Matrix \begin{bmatrix} E_{X_E}^K \otimes X_K^H & & \\ & E_{X_S}^K \otimes X_K^H & \\ & & E_{X_M}^K \otimes X_K^H \end{bmatrix} \right)^Q \cdot \frac{\theta_{\rho(t')}}{2} \right)_{E_X(t')}^{Q_{MR}} \right] \sim S_{Left, right}^{m+k-1} \left(\sum_{k \geq 3}^m S_{Left, right}^{-k+1} (Q_{MR}^{Core \ energy})_{\delta}^H \right), \text{ and } s \text{ is expressed dimension} \quad (14)$$

$Q_{MR}^{Core \ energy}$ is the core energy to maintain brain like (human brain) memory (information storage medium) [i.e. memory suspension maintenance energy]. So $S_k^{-1}(Q_{MR}^{Core \ energy})$ -cut bundle (carrying energy), $\rho_{\theta}(t'(Q_{MR}^{Core \ energy}))$ -cotangent bundle (carrying energy). $S_k^{-1}(Q_{MR}^{Core \ energy})$ -slice bundle carries a large amount of identifiable information data, which is suitable for brain like (human brain). The key group generation sequence of cotangent bundle $\rho_{\theta}(t')$ is used to extract useful information data, i.e

$$S_k^{-1}(\rho_{\theta}(t')) \xrightarrow{\text{Extract data}} \left[{}^+ \Omega_{t'(\theta)}^{S_{\partial M}^{-1}} \wedge {}^- \Omega_{t'(\theta)}^{S_{\partial M}^{-1}} \right] \quad (15)$$

${}^+\Omega_{t'(\theta)}^{S_{\partial M}^{-1}}\left(S_k^{-1}\left(\rho_{\theta}(t')\right)\right) \wedge {}^-\Omega_{t'(\theta)}^{S_{\partial M}^{-1}}\left(S_k^{-1}\left(\rho_{\theta}(t')\right)\right)$ is the extraction information data function of the sequence generated by the key group.

2. RECONSTRUCTED BRAIN LIKE NEURAL NETWORK R-KFDNN

R-KFDNN Neuron structure function: ${}^+\Omega_{t'(\theta)}^{S_{\partial M}^{-1}}\left(S_k^{-1}\left(\rho_{\theta}(t')\right)\right) \wedge {}^-\Omega_{t'(\theta)}^{S_{\partial M}^{-1}}\left(S_k^{-1}\left(\rho_{\theta}(t')\right)\right)$

R-KFDNN Neuron linked neural network: $\sum_{k \geq 3}^m ctg^s \left(\sum_{\rho=2}^m \rho_{\theta} \cdot \frac{\theta_{\rho(t')}}{2} \right)_{E_{X(t')}}^{Q_{MR}}$

Therefore, the functional structure of brain like neural network is reconstructed:

$${}^+\Omega_{t'(\theta)}^{S_{\partial M}^{-1}} \left(S_k^{-1} \left(\sum_{k \geq 3}^m ctg^s \left(\sum_{\rho=2}^m \rho_{\theta} \cdot \frac{\theta_{\rho(t')}}{2} \right)^{Q_E} \right) \right) \wedge {}^-\Omega_{t'(\theta)}^{S_{\partial M}^{-1}} \left(S_k^{-1} \left(\sum_{k \geq 3}^m ctg^s \left(\sum_{\rho=2}^m \rho_{\theta} \cdot \frac{\theta_{\rho(t')}}{2} \right)^{Q_E} \right) \right)$$

The above formula is the function body of local reconstruction brain like neural network of left and right brain (human brain). The following formula is the complex high-dimensional equation R-KFDNN that reconstructs the function body of the brain like (human brain) overall neural network.

$$\begin{aligned} S_{Left, right}^{m+k-1} \left[{}^+\Omega_{t'(\theta)}^{S_{\partial M}^{-1}} \left(S_k^{-1} \left(\sum_{k \geq 3}^m ctg^s \left(\sum_{\rho=2}^m \rho_{\theta} \cdot \frac{\theta_{\rho(t')}}{2} \right)^{Q_E} \right) \right) \right] &= \Omega^{k+1}[\theta(\rho(t))]_{S_{Left, right}^{m+k-1}}, \text{ and } Q_E \\ &= Matrix \left[\begin{array}{c} E_{X_E}^K \otimes X_K^H \\ E_{X_S}^K \otimes X_K^H \\ E_{X_M}^K \otimes X_K^H \end{array} \right]_i^Q \text{ is expressed core energy} \end{aligned} \quad (16)$$

The compact correlation between special flexible neural network and reconstructed brain neural network is established to solve the complexity problem in AI, and the hidden layer of KFDNN deep neural network. Slice bundle S_k^{-1} equivalent to the key group generation sequence of brain like R-KFDNN, i.e

${}^+\Omega_{t'(\theta)}^{S_{\partial M}^{-1}}\left(S_k^{-1}\left(\rho_{\theta}(t')\right)\right) \wedge {}^-\Omega_{t'(\theta)}^{S_{\partial M}^{-1}}\left(S_k^{-1}\left(\rho_{\theta}(t')\right)\right)$ is the hidden layer equivalent to KFDNN

The quasi thinking iterative programming of KFDNN is simpler and more practical than R-KFDNN in AI mathematical model. And KFDNN uses 3 sets of core formulas of depth statistics.

$$P_{(A_i, A_j)}^{(1)} = \left(\frac{1}{4}\right)^n \times \left[\sin \left(A_1 + \sum_{i=2}^m A_i + n \cdot \frac{\pi}{4} \right) + \sin \left(A_1 - \sum_{i=2}^m A_i + n \cdot \frac{\pi}{4} \right) \right]_{P_{i(x,y)}^*} \quad (17)$$

$$\begin{aligned} P_{(A,B)}^{(2)} &= \left(\frac{1}{4}\right)^{n-1} \times \sqrt{2} \left[\sin \left(\frac{A_1}{2} + \frac{\pi}{4} + n \cdot \frac{\pi}{4} \right) \cos \left(\sum_{i=2}^m A_i + \sum_{i=2}^m i \cdot \frac{A_i}{2} \right) \right. \\ &\quad \left. - \sin \left(\frac{B_1}{2} + \frac{\pi}{4} + n \cdot \frac{\pi}{4} \right) \cos \left(\sum_{i=2}^m B_i + \sum_{i=2}^m i \cdot \frac{B_i}{2} \right) \right]_{P_{ij(x_i, y_j)}^*} \end{aligned} \quad (18)$$

[Tanh \times Ctanh][∇]

$$\begin{aligned}
&= \frac{\left[\frac{k^2 \sigma_1}{\sqrt[3]{\frac{\pi^2}{4}}} \times e^{ij} \frac{1}{\theta^{\frac{1}{\sqrt{\pi}}}} \left[(X_i - i\bar{X})_i - \frac{\mu}{\sigma} \right]^3 - \frac{k^2 \sigma_2}{\sqrt[3]{\frac{\pi^2}{4}}} \times e^{ij} \frac{1}{\theta^{\frac{1}{\sqrt{\pi}}}} \left[(X_i + i\bar{X})_j - \frac{\mu}{\sigma} \right]^3 \right]}{\left[\frac{k^2 \sigma_3}{\sqrt[3]{\frac{\pi^2}{4}}} \times e^{ij} \frac{1}{\theta^{\frac{1}{\sqrt{\pi}}}} \left[(X_i - i\bar{X})_i - \frac{\mu}{\sigma} \right]^3 + \frac{k^2 \sigma_4}{\sqrt[3]{\frac{\pi^2}{4}}} \times e^{ij} \frac{1}{\theta^{\frac{1}{\sqrt{\pi}}}} \left[(X_i + i\bar{X})_j - \frac{\mu}{\sigma} \right]^3 \right]} \\
&\otimes \frac{\left[\frac{k^2 \sigma_5}{\sqrt[3]{\frac{\pi^2}{4}}} \times e^{ij} \frac{1}{\theta^{\frac{1}{\sqrt{\pi}}}} \left[(X_i - i\bar{X})_i - \frac{\mu}{\sigma} \right]^3 + \frac{k^2 \sigma_6}{\sqrt[3]{\frac{\pi^2}{4}}} \times e^{ij} \frac{1}{\theta^{\frac{1}{\sqrt{\pi}}}} \left[(X_i + i\bar{X})_j - \frac{\mu}{\sigma} \right]^3 \right]}{\left[\frac{k^2 \sigma_7}{\sqrt[3]{\frac{\pi^2}{4}}} \times e^{ij} \frac{1}{\theta^{\frac{1}{\sqrt{\pi}}}} \left[(X_i - i\bar{X})_i - \frac{\mu}{\sigma} \right]^3 - \frac{k^2 \sigma_8}{\sqrt[3]{\frac{\pi^2}{4}}} \times e^{ij} \frac{1}{\theta^{\frac{1}{\sqrt{\pi}}}} \left[(X_i + i\bar{X})_j - \frac{\mu}{\sigma} \right]^3 \right]} \\
&, \text{ and } \sigma \left(\pi, \frac{\pi}{4}, \frac{\pi}{2}, 2\pi \right)^{-T^2} \rightarrow \sigma \left(\pi, \frac{\pi}{4}, \frac{\pi}{2}, 2\pi \right)^{T^2}, \quad (19)
\end{aligned}$$

i. KFDNN is trained and learned by KNN neural network, which greatly improves the risk control accuracy of AI mathematical model.

The reconstructed brain neuron network R-KFDDN is much more difficult than the above KFDNN. Its mathematical model itself has nonlinear disturbance in high-dimensional space, and the information field data processing runs on different levels, different dimensions, different tangent bundles and cotangent bundles. Key group is needed for data extraction. There is a hidden time tangent in data guidance, which is similar to data distribution table, but more complex than it.

$$\text{Key group: } {}^{+}\Omega_{t'(\theta)}^{S_{\partial M}^{-1}} \left(S_k^{-1} \left(\rho_{\theta} (t') \right) \right) \wedge {}^{-}\Omega_{t(\theta)}^{S_{\partial M}^{-1}} \left(S_k^{-1} \left(\rho_{\theta} (t') \right) \right)$$

$$\text{Brain like high dimensional morphology: } \Omega^{k+1} [\theta(\rho(t))]_{S_{Left, right}^{m+k-1}}, \text{ Different dimensions}$$

$$\text{Different layer forms: } S_{Left, right}^{m+k-1} \left(\sum_{k \geq 3}^m ctg^s \left(\sum_{\rho=2}^m \rho_{\theta} \cdot \frac{\theta_{\rho(t')}}{2} \right)_{E_{X(t')}}^{Q_{MR}} \right)$$

$$\text{Different cut bundle morphology (slice bundle): } S_k^{-1} \left(\rho_{\theta} (t') \right)^{Q_E}$$

$$\text{Cotangent bundle form: } \rho_{\theta} \left(t' (Q_{MR}^{Core \ energy}) \right)$$

$$\text{Data guided hidden time tangent: } \rho_{\theta} \left(t' (Q_E) \right) \rightarrow \sum_{k \geq 3}^m ctg^s \left(\sum_{\rho=2}^m \rho_{\theta} \cdot \frac{\theta_{\rho(t')}}{2} \right)_{E_{X(t')}}^{Q_{MR}} \text{ is similar to the data allocation table,}$$

but more complex.

The key group is distributed on the slice bundle, i.e. ${}^{+}\Omega_{t'(\theta)}^{S_{\partial M}^{-1}} (S_k^{-1}) \wedge {}^{-}\Omega_{t(\theta)}^{S_{\partial M}^{-1}} (S_k^{-1})$, and S_k^{-1} is expressed slice bundle.

$${}^{+}\Omega_{t'(\theta)}^{S_{\partial M}^{-1}} \left(S_k^{-1} \left(\rho_{\theta} (t') \right) \right) \rightarrow \rho_{\theta} (t') \subset \sum_{k \geq 3}^m ctg^s \left(\sum_{\rho=2}^m \rho \cdot \frac{\theta_{\rho(t')}}{2} \right)_{E_{X(t')}}^{Q_E}$$

$$\text{That is, the key group should finally be distributed on the } \rho_{\theta} (t')\text{-Time tangent arc of } \sum_{k \geq 3}^m ctg^s \left(\sum_{\rho=2}^m \rho \cdot \frac{\theta_{\rho(t')}}{2} \right)_{E_{X(t')}}^{Q_E}.$$

Sometimes in the brain like (human brain), the key group may be called the memory fragment distribution table.

ii. Memory analysis and AI mathematical model analysis of brain

$$\omega^s(\lambda^i) \rightarrow {}^{+\wedge-}\Omega_{t'(\theta)}^{S_{\theta M}^{-1}}\left(S_k^{-1}(\rho_{\theta}(t'))\right), \text{ and } \lambda^i \text{ is brain wave like frequency,}$$

ω is the angular velocity and s is the dimension

$$\left[{}^{+\wedge-}\Omega_{t'(\theta)}^{S_{\theta M}^{-1}}\right]_{\rho_{\theta}}^T \sim \Omega^{s+1}\left(\frac{\omega^s(\lambda^i)}{S_k^{-1}(\rho_{\theta}(t'))}\right)$$

Introduction to memory analysis - mirror reflection (with local random data loss)

$$\begin{bmatrix} \omega^s(\lambda^i) & S_k^{-1}(\rho_{\theta}(t')) \\ s\Omega^T(\omega, S_k^{-1}) & Q_E \end{bmatrix} \sim \left[{}^{+\wedge-}\Omega_{t'(\theta)}^{S_{\theta M}^{-1}}\right]_{\rho_{\theta}}^T$$

$$\begin{bmatrix} \omega_1 & S_1^{-1} & \omega_2 & \dots & \dots & \Omega_{Q_E}^{s+1}(\lambda^i)_{\omega} \\ S_1^{-1} & \omega_2 & S_2^{-1} & \dots & \dots & \vdots \\ \vdots & \vdots & \vdots & \ddots & \ddots & \vdots \\ \rho_{\theta_1} & \rho_{\theta_2} & \dots & \dots & \dots & \vdots \\ \dots & \dots & \dots & \dots & \dots & \vdots \end{bmatrix} \xrightarrow[\text{local random data loss}]{\text{Mirror reflection}} \begin{bmatrix} \dots & \dots & \dots & \dots & \dots & \rho_{\theta_2}^* \\ \dots & \dots & \dots & \dots & \dots & \rho_{\theta_1}^* \\ \vdots & \vdots & \vdots & \vdots & \vdots & \vdots \\ \Omega_{Q_E}^{s+1}(\lambda^i)_{\omega} & \dots & \dots & S_2^{-1} & \dots & \vdots \\ \dots & \dots & \dots & \omega_2^* & S_1^{-1} & \vdots \\ \dots & \dots & \dots & \dots & \omega_1^* & \vdots \end{bmatrix} \quad (20)$$

if ${}^{+}\Omega_{Q_E}^{s+1}(\lambda^i)_{\omega} \vee {}^{-}\Omega_{Q_E}^{s+1}(\lambda^i)_{\omega} \cong I^{s+1}(\lambda^i)_{\omega}$, and s is the dimension, ω is the amplitude, λ^i or λ^i_* is the frequency.

Therefore, the key variable of memory analysis is $I^{s+1}(\lambda^i)_{\omega}$, which obtains brain like (human brain) information data through the mirror reflection of high-dimensional information field.

$$\left[{}^{+\wedge-}\Omega_{t'(\theta)}^{S_{\theta M}^{-1}}\right]_{\rho_{\theta}}^T \rightarrow \left[{}^{+}\Omega_{Q_E}^{s+1}(\lambda^i)_{\omega} \vee {}^{-}\Omega_{Q_E}^{s+1}(\lambda^i)_{\omega}\right]$$

Parsing is embedded in information and runs on a higher dimension. Memory parsing requires high speed $\omega^s(\lambda^i)$, and linear.

Memory Parsing: $I_{pass}^{s+1}(\lambda^i)_{\omega} : \left[{}^{+}\Omega_{Q_E}^{s+1}(\lambda^i)_{\omega} \vee {}^{-}\Omega_{Q_E}^{s+1}(\lambda^i)_{\omega}\right]_{\rho_{\theta}(t')}^{S_k^{-1}}$

$$\begin{aligned} I_{pass}^{s+1}(\lambda^i)_{\omega} : & \left[{}^{+}\Omega_{Q_E}^{s+1}(\lambda^i)_{\omega} \vee {}^{-}\Omega_{Q_E}^{s+1}(\lambda^i)_{\omega}\right]_{\rho_{\theta}(t')}^{S_k^{-1}} \\ & \dots \\ I_{pass}^3(\lambda^i)_{\omega} : & \left[{}^{+}\Omega_{Q_E}^3(\lambda^i)_{\omega} \vee {}^{-}\Omega_{Q_E}^3(\lambda^i)_{\omega}\right]_{\rho_{\theta}(t')}^{S_k^{-1}} \\ I_{pass}^2(\lambda^i)_{\omega} : & \left[{}^{+}\Omega_{Q_E}^2(\lambda^i)_{\omega} \vee {}^{-}\Omega_{Q_E}^2(\lambda^i)_{\omega}\right]_{\rho_{\theta}(t')}^{S_k^{-1}} \end{aligned} \quad (21)$$

The compact compression of $\rho_{\theta}(t')$, that is, the compression structure with time t' at the same time. $I_{pass}^{s+1}(\lambda^i)_{\omega}$ will

switch freely in the high-dimensional information field. Therefore, the key to memory analysis is in $I_{pass}^{s+1}(\lambda^i)_{\omega(t')}$, which

is a linear wave structure with special frequency.

3. Carry the key group generation sequence to the left and right brain kernels, and generate the key group generation sequence on each reduced $S_{\partial M}^{-1}$

3.1 Carrying key group to generate a sequence of left and right brain (brain like) kernels, generating a high-dimensional complex string bundle potential sequence in a higher dimensional power function to form high-dimensional coil. The generation sequence of the key group on each reduced $S_{\partial M}^{-1}$

i. The dual key group core potential orthogonal sliding mode for generating sequences of high-dimensional and low dimensional tangent bundle core potential key groups. The dual key group core potential generation sequence is located on the hypersurface of the main axis of the time cone, and dynamically and weakly nonlinearly rotates to generate the key group core potential [convex core] generation sequence.

$${}_{left}^+ \Omega(S_{\lambda(t,\theta)}^{-1}) \wedge {}_{right}^- \Omega(S_{\lambda(t,\theta)}^{-1}) \rightsquigarrow \left[\sin \left(\sum_{i=2}^m \rho_{\theta}^i \cdot \frac{\theta_{\rho(t')}^i}{2} \wedge \sum_{j=2}^m \rho_{\beta}^j \cdot \frac{\beta_{\rho(t')}^j}{2} \right) \otimes \cos \left(\sum_{j=2}^p \rho_{\theta}^j \cdot \frac{\theta_{\rho_*}^j(t')}{2} \wedge \sum_{i=2}^q \rho_{\beta}^i \cdot \frac{\beta_{\rho_*}^i(t')}{2} \right) \right]^{\omega(t)^{i-\omega(\theta)}}$$

${}_{left}^+ \Omega(S_{\lambda(t,\theta)}^{-1}) \wedge {}_{right}^- \Omega(S_{\lambda(t,\theta)}^{-1})$ represents the separation of the left and right hemispheres of the brain, with each slice exhibiting reduced memory suspension.

$$\left\{ \begin{array}{l} {}_{left}^+ \Omega(S_{\lambda(t,\theta)}^{-1}) \rightsquigarrow \left[\sin^2 \left(\sum_{i=2}^m \theta^i \cdot \frac{\theta_{\rho(t')}^i}{2} \right) + \cos^2 \left(\sum_{j=2}^m \theta_*^j \cdot \frac{\theta_{\rho(t')}^j}{2} \right) \right]^{\omega(t)^{i-\omega(\theta)}} \\ {}_{right}^- \Omega(S_{\lambda(t,\theta)}^{-1}) \rightsquigarrow \left[\sin^2 \left(\sum_{i=2}^m \beta^i \cdot \frac{\beta_{\rho(t')}^i}{2} \right) + \cos^2 \left(\sum_{j=2}^m \beta_*^j \cdot \frac{\beta_{\rho(t')}^j}{2} \right) \right]^{\omega(t)^{i-\omega(\theta)}} \end{array} \right.$$

ii. If the $H_{\langle f \otimes F \rangle}$ harmonic mapping is stable and flat, at the time tangent point t_i^{∇} , its core potential $a_{ii\uparrow\downarrow}^{(kk)}$ is tangent to the surface and the normal vector of the timeline intersects. And the complex variable function of \mathcal{N}_1 rotation winding around the \mathcal{N}_0 axis nonlinearly crosses the cross domain and generates a sequence period $a_{\omega=i2\pi}^{(nm)\uparrow\downarrow}$. The hidden timeline and the potential of high-dimensional generated sequences form a spatial structure of convolutional potential.

$$\langle {}^{(\theta,\beta)} \Omega_{T^2|_1^0}^{i\omega} \rangle_{\wedge \rho_{(\theta,\beta)}(t)}, \langle {}^{(\theta,\beta)} \Omega_{T^2|_0^1}^{i\omega-1} \rangle_{\wedge \rho_{(\theta,\beta)}(t)} \cdot a_{nn}^{\uparrow\downarrow} \rightsquigarrow \langle \sin \left(T^{-1} \begin{vmatrix} 0 & 1 \\ 1 & 0 \end{vmatrix} \cdot \sum_{s=3}^m \theta^s \cdot \frac{\theta_{\rho(t)}^{s-1}}{2} \right), \cos \left(T^{-1} \begin{vmatrix} 1 & 0 \\ 0 & 1 \end{vmatrix} \cdot \sum_{s=3}^m \beta^s \cdot \frac{\beta_{\rho(t)}^{s-1}}{2} \right) \rangle^{(i\omega, i\omega-1)} \cdot a_{mm}^{\uparrow\downarrow} \quad (22)$$

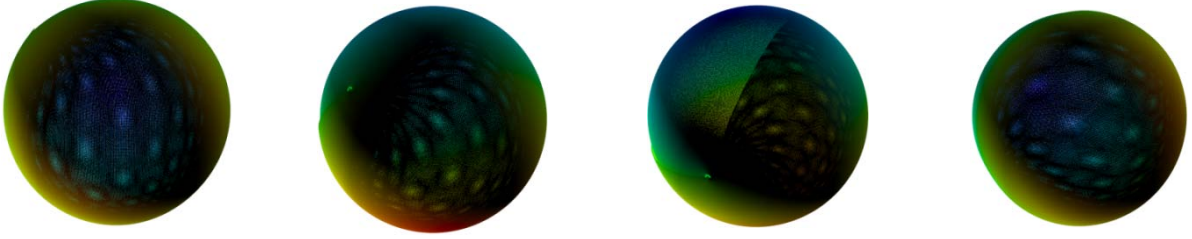


Fig04. RLLM enhances thinking ability, search, fine tune and shrink parameter group scales. The $H_{(f \otimes F)}$ harmonic mapping is stable and flat, at the time tangent point t_i^V , its core potential $a_{ii\uparrow\downarrow}^{(kk)}$ is tangent to the surface and the normal vector of the timeline intersects. And the complex variable function of \mathcal{N}_1 rotation winding around the \mathcal{N}_0 axis nonlinearly crosses the cross domain and generates a sequence period $a_{\omega=i2\pi}^{(nn)\uparrow\downarrow}$. The hidden timeline and the potential of high-dimensional generated sequences form a spatial structure of convolutional potential.

$$P_{H_{(f \otimes F)}^*}^{\partial M_{\Omega}^s} \left(\Omega^{(i\omega, i\omega-1)} \cdot Q_E^{2n}(\rho_{(\theta, \beta)}(t'))^{\pm \frac{\pi}{2} + nk\pi} \cdot a_{mm}^{\uparrow\downarrow} \right) \\ \rightsquigarrow \langle \sin^{2n} \left(T^{-1} \begin{vmatrix} 0 & 1 \\ 1 & 0 \end{vmatrix} \cdot \sum_{s=3}^m \rho_{\theta}^s \cdot \frac{\theta^{s-1}}{2} \right) \wedge \cos^{2n} \left(T^{-1} \begin{vmatrix} 1 & 0 \\ 0 & 1 \end{vmatrix} \cdot \sum_{s=3}^m \rho_{\beta}^s \cdot \frac{\beta^{s-1}}{2} \right) \rangle^{(i\omega, i\omega-1)} \cdot a_{mm}^{\uparrow\downarrow} \quad (23)$$

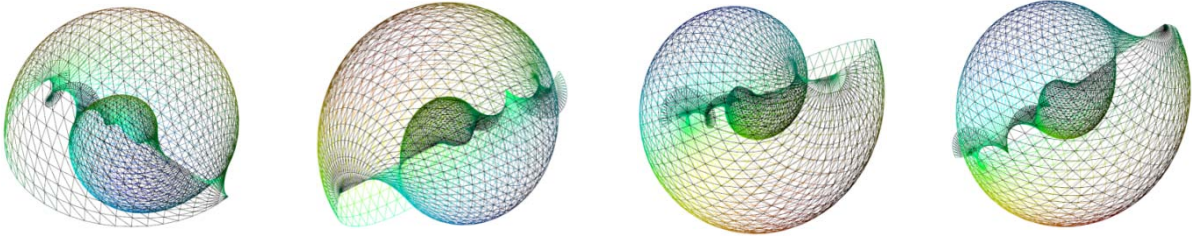


Fig05. RLLM enhances thinking ability, search, fine tune and shrink parameter group scales. The $H_{(f \otimes F)}$ harmonic mapping is stable and flat, at the time tangent point t_i^V , its core potential $a_{ii\uparrow\downarrow}^{(kk)}$ is tangent to the surface and the normal vector of the timeline intersects. And the complex variable function of \mathcal{N}_1 rotation winding around \mathcal{N}_0 axis nonlinearly crosses the cross domain and generates sequence period $a_{\omega=i2\pi}^{(nn)\uparrow\downarrow}$. The hidden timeline and the potential of high-dimensional generated sequences form a spatial structure of convolutional potential.

iii. The perception image of the brain like eye is equivalent to $MR^{H_{ij} Q_i H_{ji}^H}$, projected onto the high-dimensional key table Ω^{K+1} of the dual key group.

$$\langle \cos \left(T^{-1} \begin{vmatrix} 1 & 0 \\ 0 & 1 \end{vmatrix} \cdot \sum_{s=3}^m \beta^s \cdot \frac{\beta^{s-1}}{2} \right) \rangle^{(i\omega, i\omega-1)}, \text{ and } s = 2, \omega - 1, \omega = 1.5$$

$$\Omega^{K+1}[\langle \theta, \beta \rangle(\rho(t))]_{S_{Left, right}^{m+k-1}}^{Q_{MR}} = \Omega^{K+1} \left[\langle \theta, \beta \rangle \left(\rho_t \left(\sum \frac{\delta}{\omega_i} \times \log |I + R^{-1} \times H_{ij} \times Q_{MR}^{Core \ energy} \times H_{ji}^H| \right) \right) \right], \text{ and}$$

R^{-1} Interference signal

iv. Generate sequences for dual key group using the cotangent surface of the projection slice

$S_K^{-1} \left(MR^{H_{ij} Q_i H_{ji}^H} \right)$ or $S_K^{-1} \left(Brain^{H_{ij} Q_i H_{ji}^H} \right)$ high-dimensional hyperspace, which carries the energy aware image projection and its essential perception of the energy fluctuation distribution of the image. If it needs to be translated into a cognitive information system, the following equation can be used.

$$\left[+\Omega_t^{(S_{\partial M}^{-1})} \left(S_K^{-1} \left(\sum_{K \geq 3}^m ctg^s \left(\sum_{\rho=2}^m \rho_\theta \cdot \frac{\theta_{\rho(t)}}{2} \right)^{Q_E} \right) \vee -\Omega_t^{(S_{\partial M}^{-1})} \left(S_K^{-1} \left(\sum_{K \geq 3}^m ctg^s \left(\sum_{\rho=2}^m \rho_\beta \cdot \frac{\beta_{\rho(t)}}{2} \right)^{Q_E} \right) \right) \right] \leftarrow$$

$$\Omega^{k+1} \left[\langle \theta, \beta \rangle \left(\rho_t \left(\sum \frac{\delta}{\omega_i} \times \log |I + R^{-1} \times H_{ij} \times Q_{MR}^{Core \ energy} \times H_{ji}^H| \right) \right) \right], \text{ and if } Q_{MR}^{Core \ energy}$$

$$= Matrix \begin{bmatrix} E_{X_E}^K \otimes X_K^H & & \\ & E_{X_S}^K \otimes X_K^H & \\ & & E_{X_M}^K \otimes X_K^H \end{bmatrix}_i^Q, R^{-1} \text{ Interference signal}$$

$$+ \vee - \Omega_t^{(S_{\partial M}^{-1})} \left[S_K^{-1} \left(\sum_{K \geq 3}^m ctg^s \left(\sum_{\rho=2}^m \rho_\theta \cdot \frac{\theta_{\rho(t)}}{2} \right) \right) \vee S_K^{-1} \left(\sum_{K \geq 3}^m ctg^s \left(\sum_{\rho=2}^m \rho_\beta \cdot \frac{\beta_{\rho(t)}}{2} \right) \right) \right] \xleftarrow{\text{Interpretation}}$$

$$\left[\langle \sin \left(T^{-1} \begin{vmatrix} 1 & 0 \\ 0 & 1 \end{vmatrix} \cdot \sum_{s=3}^m \theta^s \cdot \frac{\theta_{\rho(t)}^{s-1}}{2} \right) \vee \cos \left(T^{-1} \begin{vmatrix} 0 & 1 \\ 1 & 0 \end{vmatrix} \cdot \sum_{s=3}^m \beta^s \cdot \frac{\beta_{\rho(t)}^{s-1}}{2} \right) \rangle_{a_{mm}^{11}}^{i\omega, i\omega-1} \right]^\Sigma$$

The interpreted information is hidden in the brain like slice cluster, which is the generation sequence of the dual key group core potential (convex core).

$$\left\{ \begin{array}{l} S_K^{-1} \left(\sum_{K \geq 3}^m \frac{\cos^s \left(\sum_{s=2}^m \theta \cdot \frac{\theta_{\rho(t')}}{2} \right)}{\sin^s \left(\sum_{s=2}^m \theta \cdot \frac{\theta_{\rho(t')}}{2} \right)} \right)^{Q_E} \xrightarrow[\sup]{\text{Interpretation}} \sin^{i\omega, i\omega-1} \langle \sum_{s=3}^m \theta^s \cdot \frac{\theta_{\rho(t)}^{s-1}}{2} \cdot \langle T^{-1} \begin{vmatrix} 1 & 0 \\ 0 & 1 \end{vmatrix}, T^{-1} \begin{vmatrix} 0 & 1 \\ 1 & 0 \end{vmatrix} \rangle \rangle_{a_{mm}^{11}} \\ S_K^{-1} \left(\sum_{K \geq 3}^m \frac{\cos^s \left(\sum_{s=2}^m \beta \cdot \frac{\beta_{\rho(t')}}{2} \right)}{\sin^s \left(\sum_{s=2}^m \beta \cdot \frac{\beta_{\rho(t')}}{2} \right)} \right)^{Q_E} \xrightarrow[\sup]{\text{Interpretation}} \cos^{i\omega, i\omega-1} \langle \sum_{s=3}^m \beta^s \cdot \frac{\beta_{\rho(t)}^{s-1}}{2} \cdot \langle T^{-1} \begin{vmatrix} 1 & 0 \\ 0 & 1 \end{vmatrix}, T^{-1} \begin{vmatrix} 0 & 1 \\ 1 & 0 \end{vmatrix} \rangle \rangle_{a_{mm}^{11}} \end{array} \right.$$

The above dual key group core potential (convex core) generates sequence to interpret the cognitive information system in the brain slice cluster.

vi. The mathematical model basis for generating sequences of dual key groups [core potentials] for reconstructing brain like neural networks.

Fitting a reconstructed morphological model of damaged neuromorphic (meta) **networks**. And when the convolutional kernel randomly slides the direction gradient and enhances the thinking to the limit [vector approaching collapse], it will trigger the

reconstruction of the dual key group core potential. So when recovering memory from brain damage, it is necessary to enhance thinking (recall) in familiar scenes. Simultaneously forming two sets of core formulas.

$$\begin{aligned} \langle \sin^{i\omega} \left(T^{-1} \begin{vmatrix} 1 & 0 \\ 0 & 1 \end{vmatrix} \cdot \sum_{s=3}^m \theta^s \cdot \frac{\theta_{\rho(t)}^{s-1}}{2} \right) \rangle_{a_{nn}^{\uparrow l}}^{\nabla(\omega, T)} \\ \rightsquigarrow \langle \sin^{i\omega_*} \left(T^{-1} \begin{vmatrix} 1 & 0 \\ 0 & 1 \end{vmatrix} \cdot \sum_{s=3}^m \theta^s \cdot \frac{\theta_{\rho(t)}^{s-1}}{2} \right) \vee \cos^{i\omega-1} \left(T^{-1} \begin{vmatrix} 0 & 1 \\ 1 & 0 \end{vmatrix} \cdot \sum_{s=3}^m \beta^s \cdot \frac{\beta_{\rho(t)}^{s-1}}{2} \right) \rangle_{a_{mm}^{\uparrow l}} \end{aligned} \quad (24)$$

$$\begin{aligned} \langle \sin^{i\omega} \left(T^{-1} \begin{vmatrix} 1 & 0 \\ 0 & 1 \end{vmatrix} \cdot \sum_{s=3}^m \theta^s \cdot \frac{\theta_{\rho(t)}^{s-1}}{2} \right) \rangle_{a_{nn}^{\uparrow l}}^{\nabla(\omega, T)} \\ \rightsquigarrow \langle \sin^{i\omega_*} \left(T^{-1} \begin{vmatrix} 1 & 0 \\ 0 & 1 \end{vmatrix} \cdot \sum_{s=3}^m \theta^s \cdot \frac{\theta_{\rho(t)}^{s-1}}{2} \right) \text{ or } \cos^{i\omega-1} \left(T^{-1} \begin{vmatrix} 0 & 1 \\ 1 & 0 \end{vmatrix} \cdot \sum_{s=3}^m \beta^s \cdot \frac{\beta_{\rho(t)}^{s-1}}{2} \right) \rangle_{a_{mm}^{\uparrow l}} \end{aligned} \quad (25)$$

During the process of recovering memory from brain damage, energy increases with the enhancement of thinking.

$$\begin{aligned} \left\{ \begin{aligned} & \Omega_{Q_E^2(\rho_{(\theta, \beta)}(t'))_t}^{(i\omega, i\omega-1)} \rightsquigarrow \left[S_K^{-1} \left(ctg^s \left(\sum_{\rho=2}^m \rho_{\theta} \cdot \frac{\theta_{\rho(t')}}{2} \right) \right)^{Q_E} \vee S_K^{-1} \left(ctg^s \left(\sum_{\rho=2}^m \rho_{\beta} \cdot \frac{\beta_{\rho(t')}}{2} \right) \right)^{Q_E} \right]_{normal}^{\Sigma} \\ & \text{damaged } \Omega_{Q_E^2(\rho_{(\theta, \beta)}(t'))_t}^{(i\omega, i\omega-1)} \rightsquigarrow \left[S_K^{-1} \left(ctg \left(\sum_{\rho=2}^m \rho_{\theta} \cdot \frac{\theta_{\rho(t')}}{2} \right) \right)^{Q_E} \vee S_K^{-1} \left(ctg \left(\sum_{\rho=2}^m \rho_{\beta} \cdot \frac{\beta_{\rho(t')}}{2} \right) \right)^{Q_E} \right]_{normal}^{(i\omega, i\omega-1)} \end{aligned} \right\} \quad (26) \\ \text{damaged } \Omega_{Q_E^2(\rho_{(\theta, \beta)}(t'))_t}^{(i\omega, i\omega-1)} > \Omega_{Q_E^2(\rho_{(\theta, \beta)}(t'))_t}^{(i\omega, i\omega-1)} \end{aligned}$$

vii. From the above content, it can be seen that the "RLLM Multimodal Predictive Thinking Enhanced Shrinkage Parameter Group, Scale New Generation Generative Artificial Intelligence Reconstructed Brain Neural Network R-KFDNN, and Key Group Generation Sequence" generates sequences from dual key groups to dual key group core potential generation sequences. And when the core potential (convex core) is damaged, its implicit dual (backup) key group generation sequence is obtained.

$$\begin{aligned} \langle \sin^{i\omega} \left(T^{-1} \begin{vmatrix} 1 & 0 \\ 0 & 1 \end{vmatrix} \cdot \sum_{s=3}^m \theta^s \cdot \frac{\theta_{\rho(t)}^{s-1}}{2} \right) \rangle_{a_{nn}^{\uparrow l}}^{\nabla(\omega, T)} \\ \rightsquigarrow \langle \sin^{i\omega_*} \left(T^{-1} \begin{vmatrix} 1 & 0 \\ 0 & 1 \end{vmatrix} \cdot \sum_{s=3}^m \theta^s \cdot \frac{\theta_{\rho(t)}^{s-1}}{2} \right) \text{ or } \cos^{i\omega-1} \left(T^{-1} \begin{vmatrix} 0 & 1 \\ 1 & 0 \end{vmatrix} \cdot \sum_{s=3}^m \beta^s \cdot \frac{\beta_{\rho(t)}^{s-1}}{2} \right) \rangle_{a_{mm}^{\uparrow l}}, \text{ and } \beta^s \rightsquigarrow \theta^s \end{aligned} \quad (27)$$

There exists an implicit dual key group generation sequence, i.e

$$\begin{aligned} \langle \sin^{i\omega} \left(T^{-1} \begin{vmatrix} 1 & 0 \\ 0 & 1 \end{vmatrix} \cdot \sum_{s=3}^m \theta^s \cdot \frac{\theta_{\rho(t)}^{s-1}}{2} \right) \rangle_{a_{nn}^{\uparrow l}}^{\nabla(\omega, T)} \\ \rightsquigarrow \langle \sin^{i\omega_*} \left(T^{-1} \begin{vmatrix} 1 & 0 \\ 0 & 1 \end{vmatrix} \cdot \sum_{s=3}^m \theta^s \cdot \frac{\theta_{\rho(t)}^{s-1}}{2} \right) \vee \cos^{i\omega-1} \left(T^{-1} \begin{vmatrix} 0 & 1 \\ 1 & 0 \end{vmatrix} \cdot \sum_{s=3}^m \beta^s \cdot \frac{\beta_{\rho(t)}^{s-1}}{2} \right) \rangle_{a_{mm}^{\uparrow l}}, \text{ and } \beta^s \rightsquigarrow \theta^s \end{aligned} \quad (28)$$

The sequence for generating the implicit dual key group in the above equation. $\sin^{i\omega_*} \left(T^{-1} \begin{vmatrix} 1 & 0 \\ 0 & 1 \end{vmatrix} \cdot \sum_{s=3}^m \theta^s \cdot \frac{\theta_{\rho(t)}^{s-1}}{2} \right)$

viii. The dual key group generation sequence for enhanced thinking requires an increase in thinking (energy) to enable local memory recovery in damaged brain slices. The formation of convolutional kernels is the first condition. The enhancement of thinking (energy) leads to collapse, causing the direction gradient vector to undergo reverse operations. which $T^{-1} \begin{vmatrix} 1 & 0 \\ 0 & 1 \end{vmatrix} \rightsquigarrow T^{-1} \begin{vmatrix} 0 & 1 \\ 1 & 0 \end{vmatrix}$ or $T^{-1} \begin{vmatrix} 0 & 1 \\ 1 & 0 \end{vmatrix} \rightsquigarrow T^{-1} \begin{vmatrix} 1 & 0 \\ 0 & 1 \end{vmatrix}$ is the second condition. This will gradually form the generation sequence of the dual key group core potential (convex core), which reconstructs the brain like neural network.

$$\begin{cases} \left[\text{left}^+ \Omega(S_{\lambda(t, \theta, \beta)}^{-1}) \rightsquigarrow \sin \left[\sum_{s=2}^m \rho_{\theta}^s \cdot \frac{\theta_{\rho(t)}^s}{2} \wedge \sum_{s=2}^m \rho_{\beta}^s \cdot \frac{\beta_{\rho(t)}^s}{2} \right] \right]^{\omega(t)^{i\omega(\theta)}} \\ \left[\text{right}^- \Omega(S_{\lambda(t, \theta, \beta)}^{-1}) \rightsquigarrow \cos \left[\sum_{s=2}^m \rho_{\theta}^s \cdot \frac{\theta_{\rho(t)}^s}{2} \wedge \sum_{s=2}^m \rho_{\beta}^s \cdot \frac{\beta_{\rho(t)}^s}{2} \right] \right]^{\omega(t)^{i\omega(\theta)}} \end{cases}$$

Higher dimensional power function complex string bundle potential generation sequence carrying a brain like slice bundle energy structure key group generation sequence. And during the process of recovering memory from brain damage, energy increases with thinking.

This formula is a separation of the left and right hemispheres of the brain, with each slice being reduced in memory suspension.

According to $\theta^i \cdot \frac{\theta_{\rho(t)}^i}{2} = 1/t \times \theta_{\rho}^{i-1} \times \theta^i = 1/t \times \theta_{\rho}^{i-1} \times \theta^i = \frac{1}{t} \cdot \theta_{\rho}^i$, So the above equation can be written as

$$\begin{cases} \left[\text{left}^+ S_{\lambda(t, \theta)}^{-1} \rightsquigarrow \left[\sin^2 \left(\sum_{i=2}^m \frac{1}{t} \cdot \theta_{\rho}^i \right) + \cos^2 \left(\sum_{j=2}^m \frac{1}{t} \cdot \theta_{\rho}^j \right) \right]^{\omega(t)^{i\omega(\theta)}} \right] \\ \left[\text{right}^- S_{\lambda(t, \theta)}^{-1} \rightsquigarrow \left[\sin^2 \left(\sum_{i=2}^m \frac{1}{t} \cdot \beta_{\rho}^i \right) + \cos^2 \left(\sum_{j=2}^m \frac{1}{t} \cdot \beta_{\rho}^j \right) \right]^{\omega(t)^{i\omega(\theta)}} \right] \end{cases}$$

ix. The spatial distribution of energy transformation in the sequence generated by the key group [or duality] is transformed in

dimension. The final formed core distribution energy structure.

$$\begin{aligned} S_{\text{left, right}}^{m+k-1} \left[{}^+ \Omega_{t(\theta)}^{S_{\beta M}^{-1}} \left(S_K^{-1}(\rho_{\theta}(t')) \right) \vee {}^- \Omega_{t(\beta)}^{S_{\beta M}^{-1}} \left(S_K^{-1}(\rho_{\beta}(t')) \right) \right] \\ \rightsquigarrow \left[\left\langle \cos \left(T^{-1} \begin{vmatrix} 1 & 0 \\ 0 & 1 \end{vmatrix} \cdot \sum_{s=3}^m \theta^s \cdot \frac{\theta_{\rho(t)}^{s-1}}{2} \right) \vee \cos \left(T^{-1} \begin{vmatrix} 0 & 1 \\ 1 & 0 \end{vmatrix} \cdot \sum_{s=3}^m \beta^s \cdot \frac{\beta_{\rho(t)}^{s-1}}{2} \right) \right\rangle_{a_{mm}^{11}} \right]_{S_K^{-1}(t')} \end{aligned}$$

$$\text{lef, right}^+ \Omega(S_{K(t, \theta, \beta)}^{-1})_{\omega_{i\omega}} \sim [\text{lef}^+ \Omega(S_{K(t, \theta, \beta)}^{-1}) \vee \text{right}^- \Omega(S_{K(t, \theta, \beta)}^{-1})]$$

$$_{lef, right}^{+V-} \Omega(S_{K(t,(\theta, \beta))}^{-1})^{\omega^{i\omega}} \rightsquigarrow \left[\sin \left[T^{-1} \begin{vmatrix} 1 & 0 \\ 0 & 1 \end{vmatrix} \cdot \sum_{s=2}^m \rho_{\theta}^s \cdot \frac{\theta_{\rho(t)}^s}{2} \right] \wedge \cos \left[T^{-1} \begin{vmatrix} 0 & 1 \\ 1 & 0 \end{vmatrix} \cdot \sum_{s=2}^m \rho_{\beta}^s \cdot \frac{\beta_{\rho(t)}^s}{2} \right] \right]_{S_K^{-1}}^{\omega^{i\omega}(\theta, \beta)}$$

Regarding the key group generation sequence $S_{K(t,(\theta, \beta))}^{-1}$, and the key group core potential (convex core) $S_K^{-1}(\rho_{\theta}(t'))$

$$S_{lef, right}^{m+k-1} \left[{}^{+V-} \Omega_{t'(\theta, \beta)}^{S_{\theta M}^{-1}} \left(S_K^{-1}(\rho_{(\theta, \beta)}(t')) \right) \right]_{S_K^{-1}(t')} \rightsquigarrow \Omega^{k+1} \left[\langle \theta, \beta \rangle \left(\rho_t \left(\sum \frac{\delta}{\omega_i} \times \log |I + R^{-1} \times H_{ij} \times Q_{MR}^{Core \ energy} \times H_{ji}^H| \right) \right) \right] \quad (29)$$

$S_{K(t,(\theta, \beta))}^{-1}$ generates sequence of key groups primarily carrying energy, $S_K^{-1}(\rho_{\theta}(t'))$ generates sequence of key group potentials carrying convex core, and $S_K^{-1}(t')$ has MR imaging projection. It is a cognitive knowledge system formed by the high-low dimensional distribution of human class communication $Q_{MR}^{Core \ energy}$ core energy generated by nuclear potential generation sequence.

$$_{lef, right}^{+V-} \Omega(S_{K(t,(\theta, \beta))}^{-1})^{\omega^{i\omega}} \rightsquigarrow \left[\sin \left[T^{-1} \begin{vmatrix} 1 & 0 \\ 0 & 1 \end{vmatrix} \cdot \sum_{s=2}^m \rho_{\theta}^s \cdot \frac{\theta_{\rho(t)}^s}{2} \right] \wedge \cos \left[T^{-1} \begin{vmatrix} 0 & 1 \\ 1 & 0 \end{vmatrix} \cdot \sum_{s=2}^m \rho_{\beta}^s \cdot \frac{\beta_{\rho(t)}^s}{2} \right] \right]_{S_K^{-1}}^{\omega^{i\omega}(\theta, \beta)} \quad (30)$$

This formula is a separation of the left and right hemispheres of the brain, with each slice being reduced in memory suspension. The generation sequence $S_{k(t,(\theta, \beta))}^{-1}, S_K^{-1}(\rho_{\theta}(t'))$ of the key group carrying energy as the main component is the generation sequence of the core potential of the key group carrying convex core. $S_K^{-1}(t')$ has MR projection.

$$S_{Left, right}^{m+k-1} \left[{}^{+V-} \Omega_{t'(\theta, \beta)}^{S_{\theta M}^{-1}} \left(S_{K(\rho_{(\theta, \beta)}(t'))}^{-1} \right) \right]_{S_K^{-1}(t')} \rightsquigarrow \left[\Omega^{k+1} \langle \theta, \beta \rangle \left(\rho_t \left(\sum \frac{\delta}{\omega_i} \times \log |I \times R^{-1} \times H_{ij} \times Q_{MR}^{Core \ energy} \times H_{ji}^H| \right) \right) \right]$$

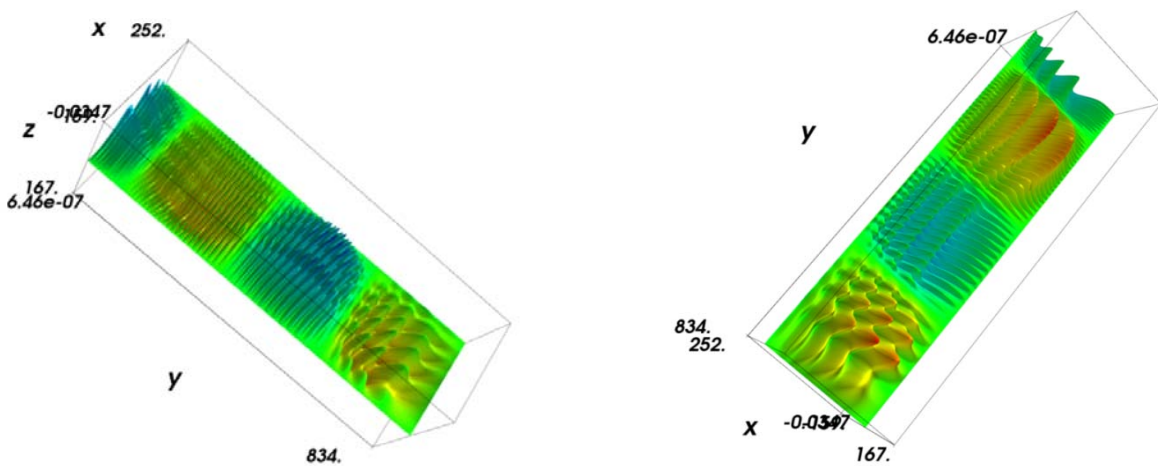


Fig06. The generation sequence of the key group to George Cantor conjecture - RLLM enhances thinking ability and search enhancement. Fine tune and shrink the parameter group scale to generate a high-dimensional complex string bundle potential generation sequence using a higher dimensional power function.

Generate sequence for the password table of the dual key group. $\langle \text{Cos} \left(T^{-1} \begin{vmatrix} 1 & 0 \\ 0 & 1 \end{vmatrix} \cdot \sum_{s=3}^m \beta^s \cdot \frac{\beta_{\rho(t)}^{s-1}}{2} \right) \rangle^{(i\omega, i\omega-1)} \cdot a_{nn}^{\uparrow\downarrow}$, and $s = 2, \omega - 1, \omega = 1.5$



Fig07. Generate sequence of dual key group core potential **and** convex kernel [password table].

$$\langle \text{Sin} \left(T^{-1} \begin{vmatrix} 0 & 1 \\ 1 & 0 \end{vmatrix} \cdot \sum_{s=3}^m \theta^s \cdot \frac{\theta_{\rho(t)}^{s-1}}{2} \right) \vee \text{Cos} \left(T^{-1} \begin{vmatrix} 1 & 0 \\ 0 & 1 \end{vmatrix} \cdot \sum_{s=3}^m \beta_*^s \cdot \frac{\beta_{\rho(t)}^{s-1}}{2} \right) \rangle_{a_{mm}^{\uparrow\downarrow}}^{(i\omega, i\omega-1)} \rightsquigarrow a_{nn}^{\uparrow\downarrow},$$

When the generation sequence of the dual key group core potential **and** **convex core** cipher table reaches a higher dimensional key table of the dual key group, a first-order energy and direction vector will be generated each time.

$$Q_E^2(\rho_{(\theta, \beta)}(t')) \sim \langle \text{Sin} \left(\frac{1}{t_1} \cdot \sum_{s=3}^m \theta^s \cdot \frac{\theta_{\rho(t)}^{s-1}}{2} \right) \wedge \text{Cos} \left(\frac{1}{t_2} \cdot \sum_{s=3}^m \beta_*^s \cdot \frac{\beta_{\rho(t)}^{s-1}}{2} \right) \rangle_{a_{mm}^{\uparrow\downarrow}}^{(i\omega, i\omega-1)}$$



Fig08. high-dimensional key group of dual key groups [high-dimensional key table].

x. Brain like (brain) slice bundle energy, left and right brain structure $_{lef, right}^{+v-} \Omega(S_{K(t, (\theta, \beta))}^{-1})^{\omega i\omega}$, and slice bundle nucleus potential (convex core)

$$S_{left, right}^{m+k-1} \left[{}^{+v-} \Omega_{t(\theta, \beta)}^{S_{\partial M}^{-1}} \left(S_K^{-1}(\rho_{(\theta, \beta)}(t')) \right) \right]_{S_K^{-1}(t')}, \text{ if } \omega i\omega \rightsquigarrow m+k-1, \text{ then}$$

$$S_{left, right}^{m+k-1} \left[{}^{+v-} \Omega_{t(\theta, \beta)}^{S_{\partial M}^{-1}} \left(S_K^{-1}(\rho_{(\theta, \beta)}(t')) \right) \right]_{S_K^{-1}(t')} \leftarrow {}_{lef, right}^{+v-} \Omega(S_{K(t, (\theta, \beta))}^{-1})^{\omega i\omega}_{S_K^{-1}(t)}, S_{left, right}^{m+k-1}$$

Core brain_like (brain) slice bundle with all brain functions. The core energy of neuronal convex core is formed by the fluctuation energy of neurons in brain like slices. And the key group generation sequence is subjected to MR projection, and the parsing process is the cognitive science system of high-low dimensional dual key group core potential (convex core) interpretation.

$$\begin{aligned}
& \langle_{left, right}^{+V-} \Omega(S_{K(t, \theta, \beta)}^{-1})^{\omega_{i\omega}} \Omega^{k+1} \left[\langle \theta, \beta \rangle \left(\rho_t \left(\sum \frac{\delta}{\omega_i} \times \log |I + R^{-1} \times H_{ij} \times Q_{MR}^{Core \ energy} \times H_{ij}^H \right) \right) \right] \rangle \\
& \rightsquigarrow S_{left, right}^{m+k-1} \left[{}^{+V-} \Omega_{t'(\theta, \beta)}^{S_{\partial M}^{-1}} \left(S_K^{-1} \left(\rho_{(\theta, \beta)}(t') \right) \right) \right]_{S_K^{-1}(t')}^{core \ potential \ [convex \ core] \ Knowledge \ [interpretation]}
\end{aligned} \tag{31}$$

$$\begin{aligned}
& S_{left, right}^{m+k-1} \left[{}^{+V-} \Omega_{t'(\theta)}^{S_{\partial M}^{-1}} \left(S_K^{-1} \left(\rho_{\theta}(t') \right) \right) \vee {}^{-V-} \Omega_{t'(\beta)}^{S_{\partial M}^{-1}} \left(S_K^{-1} \left(\rho_{\beta}(t') \right) \right) \right] \\
& \rightsquigarrow \left[\langle \cos \left(T^{-1} \begin{vmatrix} 1 & 0 \\ 0 & 1 \end{vmatrix} \cdot \sum_{s=3}^m \theta^s \cdot \frac{\theta_{\rho(t)}^{s-1}}{2} \right) \vee \cos \left(T^{-1} \begin{vmatrix} 1 & 0 \\ 0 & 1 \end{vmatrix} \cdot \sum_{s=3}^m \beta^s \cdot \frac{\beta_{\rho(t)}^{s-1}}{2} \right) \rangle_{a_{mm}^{11}}^{(i\omega, i\omega-1)} \right]_{S_K^{-1}(t')} \tag{32}
\end{aligned}$$

$$S_{left, right}^{m+k-1} \left[{}^{+V-} \Omega_{t'(\theta, \beta)}^{S_{\partial M}^{-1}} \left(S_K^{-1} \left(\rho_{(\theta, \beta)}(t') \right) \right) \right]_{S_K^{-1}(t')}^{core \ potential \ [convex \ core]}$$

3.2 RLLM multimodal predictive thinking enhanced shrinkage parameter group, Scale new generation generative artificial intelligence reconstructed brain neural network R-KFDNN and key group generation sequence MR projection

$$S_{Left, right}^{m+k-1} \left[{}^{+V-} \Omega_{t'(\theta, \beta)}^{S_{\partial M}^{-1}} \left(S_K^{-1} \left(\rho_{(\theta, \beta)}(t') \right) \right) \right]_{S_K^{-1}(t')} \Leftarrow \left[\Omega^{k+1} \langle \theta, \beta \rangle \left(\rho_t \left(\sum \cdot \frac{\delta}{\omega_i} \times \log |I \times R^{-1} \times H_{ij} \times Q_{MR}^{Core \ energy} \times H_{ij}^H \right) \right) \right]$$

$$S_{Left, right}^{m+k-1} \left[{}^{+V-} \Omega_{t'(\theta, \beta)}^{S_{\partial M}^{-1}} \left(S_K^{-1} \left(\rho_{(\theta, \beta)}(t') \right) \right) \right]_{S_K^{-1}(t')}^{core \ potential \ [convex \ core]} \tag{33},$$

$$\left[\Omega^{k+1} \langle \theta, \beta \rangle \left(\rho_t \left(\sum \cdot \frac{\delta}{\omega_i} \times \log |I \times R^{-1} \times H_{ij} \times Q_{MR}^{Core \ energy} \times H_{ij}^H \right) \right) \right] \tag{34}$$

$$\begin{aligned}
& {}_{left}^{+} \Omega(S_{\lambda(t, \theta)}^{-1}) \wedge {}_{right}^{-} \Omega(S_{\lambda(t, \theta)}^{-1}) \\
& \rightsquigarrow \left[\sin \left(\sum_{i=2}^m \rho_{\theta}^i \cdot \frac{\theta_{\rho(t')}^i}{2} \wedge \sum_{j=2}^m \rho_{\beta}^j \cdot \frac{\beta_{\rho(t')}^j}{2} \right) \otimes \cos \left(\sum_{j=2}^p \rho_{\theta}^j \cdot \frac{\theta_{\rho_*}(t')}{2} \wedge \sum_{i=2}^q \rho_{\beta}^i \cdot \frac{\beta_{\rho_*}(t')}{2} \right) \right]^{\omega(t)^{i-\omega(\theta)}}
\end{aligned}$$

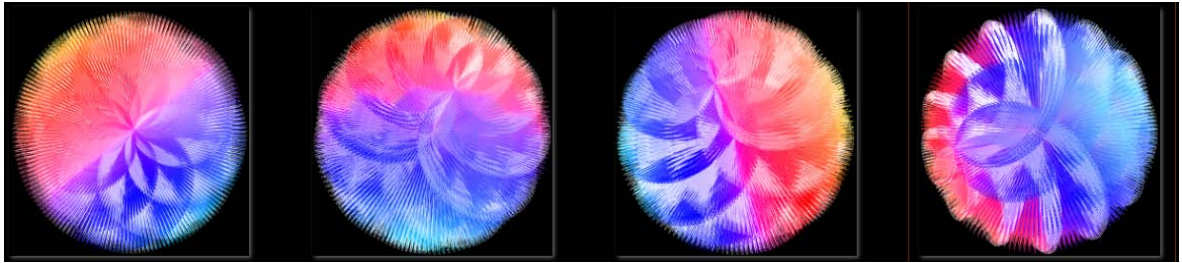


Fig09. Brain like [left and right brain] slice bundle neuron energy fluctuations.

$${}_{left, right}^{+V-} \Omega(S_{K(t, \theta, \beta)}^{-1})^{\omega(t)^{i-\omega(\theta, \beta)}} \rightsquigarrow \left[\sin \left(T^{-1} \begin{vmatrix} 0 & 1 \\ 1 & 0 \end{vmatrix} \cdot \sum_{s=2}^m \rho_{\theta}^s \cdot \frac{\theta_{\rho(t)}^{s-1}}{2} \right) \wedge \cos \left(T^{-1} \begin{vmatrix} 1 & 0 \\ 0 & 1 \end{vmatrix} \cdot \sum_{s=3}^m \rho_{\beta}^s \cdot \frac{\beta_{\rho(t)}^{s-1}}{2} \right) \right]^{\omega(t)^{i-\omega(\theta, \beta)}} \tag{35}$$

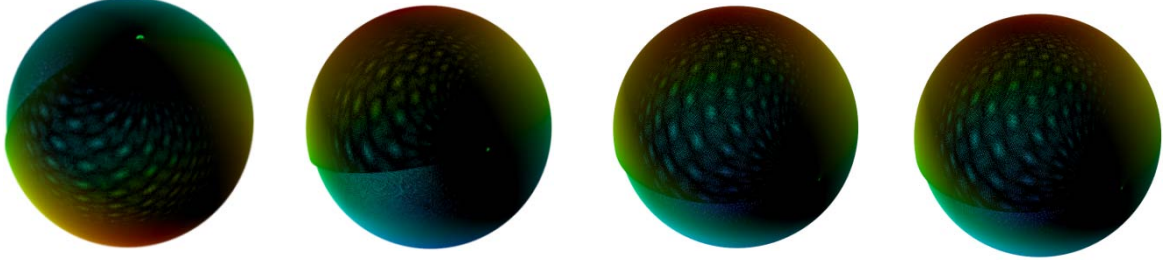


Fig10. The dual key group core potential **and** convex core carrying the key group generation sequence in the neuromorphic brain.

$$\begin{aligned} & \langle \langle \theta, \beta \rangle \Omega_{T^2}^{i\omega} \Big|_1^0 \Big|_0^1 \wedge \rho_{(\theta, \beta)}(t) \rangle, \langle \langle \theta, \beta \rangle \Omega_{T^2}^{i\omega-1} \Big|_1^0 \Big|_0^1 \wedge \rho_{(\theta, \beta)}(t) \rangle \cdot a_{nn}^{\uparrow\downarrow} \\ & \rightsquigarrow \langle \text{Sin} \left(T^{-1} \Big|_1^0 \Big|_0^1 \cdot \sum_{s=3}^m \theta^s \cdot \frac{\theta_{\rho(t)}^{s-1}}{2} \right) \vee \text{Cos} \left(T^{-1} \Big|_0^1 \Big|_1^0 \cdot \sum_{s=3}^m \beta_*^s \cdot \frac{\beta_{\rho(t)}^{s-1}}{2} \right) \rangle^{(i\omega, i\omega-1)} \cdot a_{mm}^{\uparrow\downarrow} \quad (36) \end{aligned}$$

$$\langle \text{left, right}^{+\vee-} \Omega(S_{k(t, (\theta, \beta))}^{-1})^{\omega(t)^{i\omega(\theta, \beta)}}, \Omega^{k+1} \langle \theta, \beta \rangle \left(\rho_t \left(\sum \cdot \frac{\delta}{\omega_i} \times \log |I \times R^{-1} \times H_{ij} \times Q_{MR}^{Core \text{ energy}} \times H_{ij}^H| \right) \right) \rangle, \rightsquigarrow$$

$$S_{Left, right}^{m+k-1} \left[{}^{+\vee-} \Omega_{t(\theta, \beta)}^{S_M^{-1}} \left(S_{k(\rho_{(\theta, \beta)}(t'))}^{-1} \right) \right]_{S_{k(t)}^{-1}}^{core \text{ potential } [convex \text{ core}]} \rightsquigarrow \text{Interpreting brain information and reasoning formula}$$

groups. (32)+(33)+(34)+(35)

High dimensional composite

$$\langle \text{Sin} \left(T^{-1} \Big|_1^0 \Big|_0^1 \cdot \sum_{s=3}^m \theta^s \cdot \frac{\theta_{\rho(t)}^{s-1}}{2} \right) \vee \text{Cos} \left(T^{-1} \Big|_0^1 \Big|_1^0 \cdot \sum_{s=3}^m \beta_*^s \cdot \frac{\beta_{\rho(t)}^{s-1}}{2} \right) \rangle^{(i\omega, i\omega-1)} \cdot a_{mm}^{\uparrow\downarrow}$$

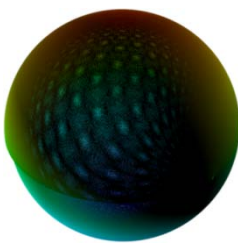
Low dimensional composite

$$\langle \text{Sin} \left(T^{-1} \Big|_1^0 \Big|_0^1 \cdot \sum_{s=3}^m \theta^s \cdot \frac{\theta_{\rho(t)}^{s-1}}{2} \right) \vee \text{Cos} \left(T^{-1} \Big|_0^1 \Big|_1^0 \cdot \sum_{s=3}^m \beta_*^s \cdot \frac{\beta_{\rho(t)}^{s-1}}{2} \right) \rangle^{(i\omega, i\omega-1)} \cdot a_{mm}^{\uparrow\downarrow},$$

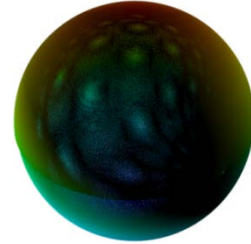
and $\langle i\omega, i\omega - 1 \rangle \rightsquigarrow 1$

High dimensional monomer

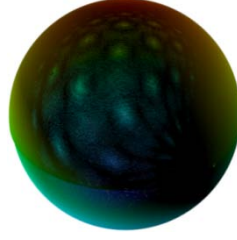
$$\langle \text{Cos} \left(T^{-1} \Big|_0^1 \Big|_1^0 \cdot \sum_{s=3}^m \beta_*^s \cdot \frac{\beta_{\rho(t)}^{s-1}}{2} \right) \rangle^{(i\omega, i\omega-1)} \cdot a_{nn}^{\uparrow\downarrow}, \text{ or } \langle \text{Cos} \left(T^{-1} \Big|_1^0 \Big|_0^1 \cdot \sum_{s=3}^m \theta^s \cdot \frac{\theta_{\rho(t)}^{s-1}}{2} \right) \rangle^{(i\omega, i\omega-1)} \cdot a_{nn}^{\uparrow\downarrow}$$



High dimensional composite normative functions



Low dimensional composite normative functions



High dimensional monomer norm

Fig11. Brain like dual key group core potential **and** convex core generation sequence, high-dimensional composite norm function and low dimensional composite norm function, as well as high-dimensional monomer norm function equation and program design type.

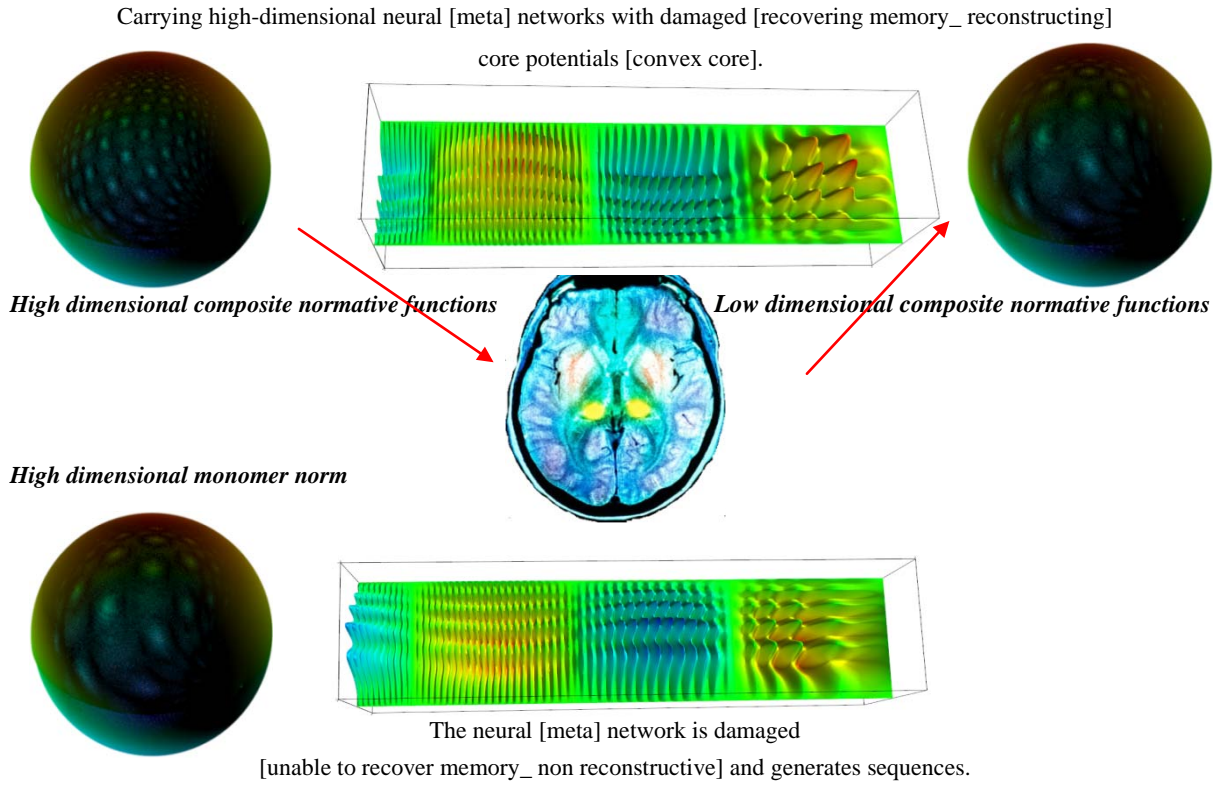


Fig12. The brain like[brain] has a high-dimensional composite dual key group core potential [convex core] generation sequence carrying high-dimensional neural damage [recovery] memory, as well as low dimensional neural damage [recovery] memory. There is a problem of local neuron information recovery and certain information loss in high-low dimensional morphology. At the same time, the generation sequence of high-dimensional monomer dual key group core potential [convex core] does not have the possibility of carrying damaged [restored] memory of high-dimensional neurons. And implement the programming model.

- i. Carrying high-dimensional neural damage [recovery] gene $\sin\left(T^{-1}\begin{vmatrix} 0 & 1 \\ 1 & 0 \end{vmatrix} \cdot \sum_{s=3}^m \theta^s \cdot \frac{\theta_{\rho(t)}^{s-1}}{2}\right)$, high-dimensional composite dual key group **core** potential [convex **core**] generation sequence; And the generation sequence of low dimensional composite dual key group **core** potential [convex **core**] for low high-dimensional nerve damage [recovery] gene $\sin\left(T^{-1}\begin{vmatrix} 0 & 1 \\ 1 & 0 \end{vmatrix} \cdot \sum_{s=3}^m \theta^s \cdot \frac{\theta_{\rho(t)}^{s-1}}{2}\right)$. This high-low dimensional morphology exhibits a lack of local neuronal information recovery. At the same

time, the generation sequence of high-dimensional monomer dual key group **core** potential [convex **core**] does not have the possibility of carrying high-dimensional neural damage [recovery] genes.

ii. Reconstructing brain like neural networks, not all neurons in brain regions can be damaged and reconstructed. Only special carrying high-dimensional neural (meta) networks can restore memory and reconstruct damaged local neurons, and form new dual key group core potential (convex core) generation sequences. So, 'RLLM Multimodal Predictive Thinking Enhanced Shrinkage Parameter Group and Scale New Generation Generative Artificial Intelligence Reconstructed Brain Neural Network R-KFDNN and Key Group Generation Sequence' carries the cutting-edge 'Cryptography of New Generation Generative Artificial Intelligence'. Thus, the reconstruction of brain like neural (meta) networks corresponds to generative AI cryptography, that is, the reconstruction structure of brain like neurons corresponding to the generation sequence of dual key group core potential [convex core], convex core potential [neurons] $a_{nn}^{\uparrow\downarrow} \rightsquigarrow a_{mm}^{\uparrow\downarrow}$.

4. The most fundamental mathematical model for the convex core morphology of new dual key group generation sequence formed by the restoration of memory and reconstruction of damaged local neurons

Mathematical model for the recovery and memory reconstruction of damaged local neurons to form a new dual key group generation sequence, convex kernel, and energy distribution.

i. The recovery of damaged local neurons requires the convex core, and more importantly, the energy fluctuations of plexiform neurons in the left and right brain slices are needed.

Local code model for program design of high-dimensional composite norm functions, generating sequence energy distribution images using a dual key group similar to a brain.

```
import numpy
from numpy import pi, sin, cos, mgrid
import numpy as np
import math
from mayavi import mlab

pi = np.pi, s=2, N=2, M=1, dphi, dtheta = pi / 250.0, pi / 250.0
[phi, theta] = mgrid[0:pi + dphi * 16/6:dphi, 0:20/6*pi + dtheta * 1.5:dtheta]
m0 = s-1; m1 = s-1; m2 = s-1; m3 = s-1; m4 = s-1; m5 = s-1; m6 = s-1; m7 = s-1;
r = numpy.power((numpy.power(np.sin(m0*phi*m1*(phi/2)+2*m0*phi*m1*(phi/2)),N) +
numpy.power(np.cos(m0*theta*m1*(theta/2)+2*m0*theta*m1*(theta/2)),N)),M)
x = r*sin(phi)*cos(theta)
y = r*cos(phi)
z = r*sin(phi)*sin(theta)
# View it.
pl = mlab.surf(x, y, z, warp_scale="auto")
mlab.axes(xlabel='x', ylabel='y', zlabel='z')
mlab.outline(pl)
```

```
mlab.show()
```

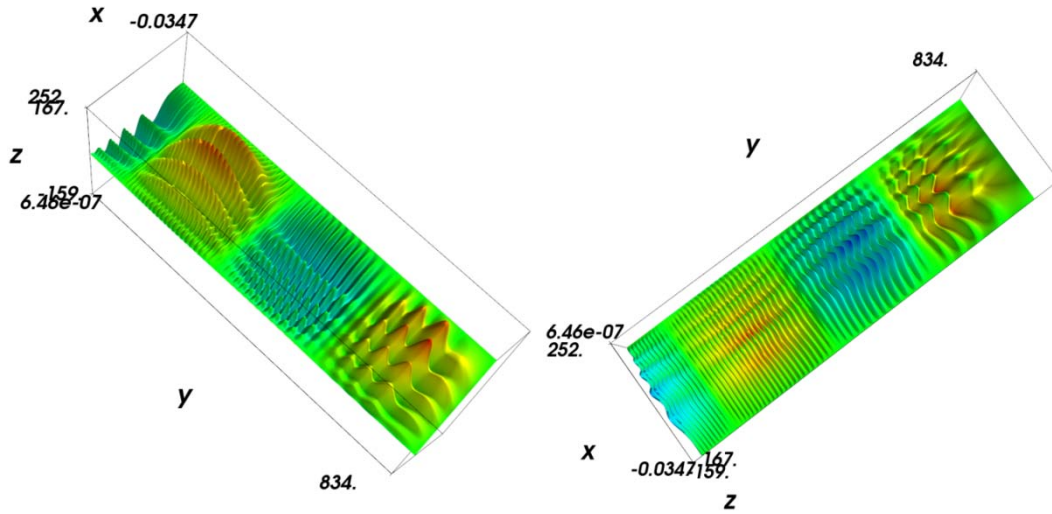


Fig13. Brain like dual key group generation sequence, high-dimensional composite norm function equation, and programming local code model.

ii. For example, in the design of high-dimensional composite function programming, a local code model [brain like] dual key group core potential [convex core] is used to generate sequence distribution images.

```
import numpy
from numpy import pi, sin, cos, mgrid
import numpy as np
import math
from mayavi import mlab

pi = np.pi, s = 2, N = 2, M = 1, t = 11, w = 22, k = 1; dphi, dtheta = pi / 250.0, pi / 250.0
[phi, theta] = mgrid[0:pi + dphi * 16/6: dphi, 0:20/6 * pi + dtheta * 1.5: dtheta]
m0 = s - 1; m1 = s - 1; m2 = s - 1; m3 = s - 1; m4 = s - 1; m5 = s - 1; m6 = s - 1; m70 = s - 1;

r = numpy.power((numpy.power(np.sin(m0 * phi * m1 * (phi/2)) + 2 * m0 * phi * m1 * (phi/2)), N)
                + numpy.power(np.cos(m0 * theta * m1 * (theta/2)) + 2 * m0 * theta * m1
                * (theta/2)), N)), M)

{x = r * sin(phi) * cos(theta)
 y = r * cos(phi)
 z = r * sin(phi) * sin(theta)}

#View it.
s = mlab.mesh(x, y, z, representation = "wireframe", line_width = 1.0)
mlab.show()
```



Fig14. Brain like dual key group core potential [convex core] generation sequence, high-dimensional composite norm function equation and local code model for programming [parameter N=2].

iii. Low dimensional composite norm function programming, local code model [brain like], dual key group, core potential [convex core], generated sequence distribution image.

```
import numpy
from numpy import pi, sin, cos, mgrid
import numpy as np
import math
from mayavi import mlab

pi = np.pi, s=3, N=1, M=1.5, t1=10, t2=20, k=s-2, dphi, dtheta = pi / 255.0, pi / 255.0
[phi, theta] = mgrid[0:pi + dphi * 16/6:dphi, 0:20/6*pi + dtheta * 1.5:dtheta]
m0 = s-2; m1 = s-2; m2 = s-1; m3 = s-1; m4 = s-1; m5 = s-1; m6 = s-1; m7 = s-1;
r = numpy.power((numpy.power(np.sin(1/t1*m1*(numpy.power(phi,k)/2)),N) +
numpy.power(np.cos(1/t2*m1*(numpy.power(theta,k)/2)),N)),M)
x = r*sin(phi)*cos(theta)
y = r*cos(phi)
z = r*sin(phi)*sin(theta)
s = mlab.mesh(x, y, z, representation="wireframe", line_width=1.0 )
mlab.show()
```



Fig15. Brain like dual key group core potential and convex core generation sequence, low dimensional composite norm function equation, and local code model for programming [parameter N=1].

iv. For example, in the design of high-dimensional monolithic norm function programs, a local code model [brain like] dual key group core potential [convex core] is used to generate sequence distribution images.

```
import numpy
from numpy import pi, sin, cos, mgrid
import numpy as np
import math
from mayavi import mlab

pi = np.pi, s=3, N=1 or N=2, M=1.5, t1=10, t2=20, k=s-2
dphi, dtheta = pi / 255.0, pi / 255.0
[phi, theta] = mgrid[0:pi + dphi * 16/6:dphi, 0:20/6*pi + dtheta * 1.5:dtheta]
m0 = s-2; m1 = s-2; m2 = s-1; m3 = s-1; m4 = s-1; m5 = s-1; m6 = s-1; m7 = s-1;
r = numpy.power((numpy.power(np.cos(1/t2*m1*(numpy.power(theta,k)/2)),N)),M)
x = r*sin(phi)*cos(theta)
y = r*cos(phi)
```

```


$$z = r \cdot \sin(\phi) \cdot \sin(\theta)$$


$$s = \text{mlab.mesh}(x, y, z, \text{representation} = \text{"wireframe"}, \text{line\_width} = 1.0)$$


$$\text{mlab.show}()$$


```

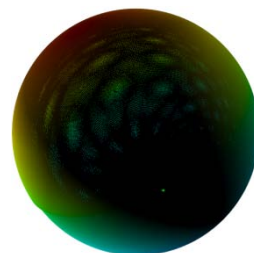
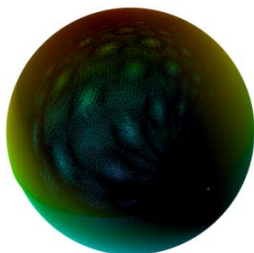


Fig16. Brain like dual key group core potential and convex core generation sequence, high-dimensional monomer norm function equation, and local code model for programming [parameter N=1].

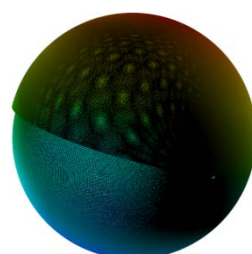
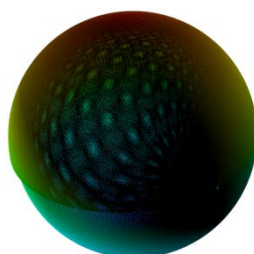


Fig17. Brain like dual key group core potential and convex core generation sequence, high-dimensional monomer norm function equation, and local code model for programming [parameter N=2].

5. CONCLUSION

Reconstruct the brain like neural network R-KFDNN, generate the sequence super tangent plane from the brain like heavy nucleus boundary key group for the first time, and fuse with the flexible depth neural network (KFDNN) and brain like neural network. From the perspective of nervous system repair of local nerve damage, this paper analyzes how the brain obtains memory analysis from the distribution table group of Time tangent bundle with fingerprint feature key group generation sequence, and so as to provide useful help for memory recovery.

REFERENCES

- [1] Zhu RongRong, Differential Incremental Equilibrium Theory, Fudan University, Vol 1, 2007:1-213
- [2] Zhu RongRong, Differential Incremental Equilibrium Theory, Fudan University, Vol 2, 2008:1-352
- [3] Liu zhuanghu, Simplicity Set Theory, Beijing China ,Peking University Press, 2001.11: 1-310
- [4] Xie bangjie, Transfinite Number and Theory of Transfinite Number, Jilin China, jilin people's publishing house, 1979.01:1-140
- [5] Nan chaoxun , Set Valued Mapping , Anhui China, Anhui University Press , 2003.04: 1-199
- [6] Li hongyan, On some Compactness and Separability in Fuzzy Topology, Chengdu China,,Southwest Jiaotong University Press, 2015.06: 1-150
- [7] Bao zhiqiang , An introduction to Point Set Topology and Algebraic Topology, Beijing China , Peking University Press, 2013.09:1-284

-
- [8] Gao hongya, Zhu yuming , Quasiregular Mapping and A-harmonic Equation, Beijing China , Science Press, 2013.03: 1-218
- [9] C. Rogers W. K. Schief, Bäcklund and Darboux Transformations: Geometry and Modern Applications in Soliton Theory, first published by Cambridge University, 2015: 1-292.
- [10] Ding Peizhu, Wang Yi, Group and its Express, Higher Education Press, 1999: 1-468.
- [11] Gong Sheng, Harmonic Analysis on Typical Groups Monographs on pure mathematics and Applied Mathematics Number twelfth, Beijing China, Science Press, 1983: 1-314.
- [12] Gu chao hao, Hu Hesheng, Zhou Zixiang, DarBoux Transformation in Soliton Theory and Its Geometric Applications (The second edition), Shanghai science and technology Press, 1999, 2005: 1-271.
- [13] Jari Kaipio Erkki Somersalo, Statistical and Computational Inverse Problems With 102 Figures, Springer.
- [14] Numerical Treatment of Multi-Scale Problems Porceedings of the 13th GAMM-Seminar, Kiel, January 24-26, 1997 Notes on Numerical Fluid Mechanics Volume 70 Edited By WolfGang HackBusch and Gabriel Wittum.
- [15] Qiu Chengtong, Sun Licha, Differential Geometry Monographs on pure mathematics and Applied Mathematics Number eighteenth, Beijing China, Science Press, 1988: 1-403.
- [16] Ren Fuyao, Complex Analytic Dynamic System, Shanghai China, Fudan University Press, 1996: 1-364.
- [17] Su Jingcun, Topology of Manifold, Wuhan China, wuhan university press, 2005: 1-708.
- [18] W. Miller, Symmetry Group and Its Application, Beijing China, Science Press, 1981: 1-486.
- [19] Wu Chuanxi, Li Guanghan, Submanifold geometry, Beijing China, Science Press, 2002: 1-217.
- [20] Xiao Gang, Fibrosis of Algebraic Surfaces, Shanghai China, Shanghai science and technology Press, 1992: 1-180.
- [21] Zhang Wenxiu, Qiu Guofang, Uncertain Decision Making Based on Rough Sets, Beijing China, tsinghua university press, 2005: 1-255.
- [22] Zheng jianhua, Meromorphic Functional Dynamics System, Beijing China, tsinghua university press, 2006: 1-413.
- [23] Zheng Weiwei, Complex Variable Function and Integral Transform, Northwest Industrial University Press, 2011: 1-396.